AN INVESTIGATION OF COPPER DISSOLUTION AND FORMATION OF INTERMETALLIC COMPOUND DURING SOLDERING

by

Mohammad Faizan

Submitted in Partial Fulfillment of the Requirements

for the Degree of

Master of Science in Engineering

in the

Civil and Environmental Engineering

Program

YOUNGSTOWN STATE UNIVERSITY
June, 2003

An Investigation of Copper Dissolution and Formation of Intermetallic Compound During Soldering

Mohammad Faizan

I hereby release this thesis to the public. I understand that this thesis will be made available from the OhioLINK ETD Center and the Maag Library Circulation Desk for public access. I also authorize the University or other individuals to make copies of this thesis as needed for scholarly research.

Signature: _______________ 07/15/03
Mohammad Faizan, Student — Date

Approvals:

_______________ 7/9/03
Dr. Guo-Xiang Wang, Thesis Advisor — Date
(University of Akron, Akron, Ohio)

_______________ 7/10/03
Dr. Robert A. McCoy, Thesis Co-Advisor — Date

_______________ 7/3/03
Dr. Javed Alam, Committee Member — Date

_______________ 7/18/03
Dr. Elvin B. Shields, Committee Member — Date

_______________ 7/23/03
Peter J. Kasvinsky, Dean of Graduate Studies — Date

ABSTRACT

Soldering is the predominant and established technique in electronic packaging industry for joining electronic components. During soldering of (Sn-rich solders), a Sn-Cu interaction takes place at the Cu/solder interface. Copper is dissolved into molten solders and subsequently the intermetallic compound (IMC) would be formed at the interface as well as in the solder matrix. Understanding of copper dissolution and the growth of IMC at the Cu/solder interface is critical in achieving reliable soldered joints. This thesis presents an experimental investigation of Cu-Sn interaction kinetics. Two types of experiments, dipping and reflow have been performed. In dipping experiments, copper (99.9% pure) samples, coated with RMA flux, were dipped vertically in molten solders. In reflow experiments, solder buttons were reflowed in furnace. The dwell time (time for which the molten solder remains in contact with the substrate) in these experiments ranged from 5 seconds to 10 minutes. The experiment temperature varied from the melting point of the solder up to 300 °C. The samples were then cut, cleaned and cold mounted in epoxy at room temperature. Regular grinding, polishing, etching, and optical metallurgical process was utilized through all samples. The average thickness of IMC and thickness reduction in copper substrates was then measured from the optical microscopy photographs. Experimental results indicated that the temperature of molten solder and the dwell time controlled the copper dissolution rate and growth of IMC at the interface. For a given process temperature, the dissolution rate of copper into solder, showed a rising trend with increasing dwell time. The rate of formation of IMC layer revealed a similar trend. The experimental data can be used to estimate the kinetics of copper dissolution and the thickness of the resulting IMC formed during soldering.

ACKNOWLEDGEMENTS

I would like to extend my sincere thanks and regards to my advisors, Dr. G.-X Wang of the University of Akron and Dr. Robert C. McCoy of the Youngstown State University and other committee members for their support and guidance during my research and compilation of this thesis.

I feel obliged to thank Dr. Scott C. Martin, Chairman of the Civil and Environmental Engineering Department for his never ending support and positive advice whenever I needed during my stay at the Youngstown State University. I express my utter gratitude to Dr. Shakir Husain of the Civil and Environmental Engineering Department for his precious guidance. Sincere regards are due to my fellow researcher, Dechao Lin of the University of Akron, for his important technical help and guidance in bringing out this research. I am very much grateful to the Department Secretary, Linda Adavasio for her prompt response to every request I made regarding my academic needs.

Exceptional thanks to my caring sister, Zamarrud, wonderful wife, Firdaus and lovely daughter Zahra for their everlasting love, encouragement and support.

TABLE OF CONTENTS

ABSTRACT iii

ACKNOWLEDGEMENTS iv

TABLE OF CONTENTS v

LIST OF FIGURES vii

LIST OF TABLES x

CHAPTER 1: INTRODUCTION 1

1.1 Objective of the Study 2

CHAPTER 2: LITERATURE REVIEW

2.1 Soldering Process 3

2.1.1 Reflow Soldering 3

2.1.2 Wave Soldering 4

2.2 Solder Materials 5

2.2.1 Factors Governing the Choice of Solder 7

2.2.1.1 Environmental Concerns 7

2.2.1.2 Process Conditions 8

2.2.1.3 Wetting 8

2.2.1.4 Reliability and Cost 9

2.3 Soldered Joint 12

2.3.1 Intermetallic Compound Layer 12

2.3.1.1 Morphology of Intermetallic Layer 16

2.3.2 Dissolution of Copper 16

2.4 Kinetics of Copper Dissolution and IMC growth 17

CHAPTER 3: EXPERIMENTAL PROCEDURES

3.1 Materials and soldering Procedures 19

3.1.1 Dipping Experiments 19

3.1.2 Reflow Experiments 22

3.2 Metallography 24

CHAPTER 4: ANALYSIS OF OBSERVED IMC GROWTH

4.1 Dipping Process 29

4.2 Reflow Process 43

4.3 Morphology of Intermetallic Compound 56

4.4 Effect of Type of Process on IMC Growth 57

CHAPTER 5: COPPER DISSOLUTION DURING THE PROCESS

5.1 Dipping Process 59

5.2 Reflow Process 62

5.3 Effect of Type of Process on Copper Dissolution 65

5.4 Effect of Solder Composition on Copper Dissolution 65

CHAPTER 6: KINETIC ANALYSIS OF GROWTH AND DISSOLUTION DATA

6.1 Kinetics of Intermetallic Compound Growth 69

6.2 Kinetics of Copper Dissolution 75

CHAPTER 7: CONCLUSIONS 79

CHAPTER 8: SCOPE FOR FURTHER WORK 80

REFERENCES 81

List of Figures

Figure Title	Page
Figure 2.1: Schematic diagram showing the principle of reflow soldering	4
Figure 2.2: Schematic diagram showing the sequence of wave soldering	5
Figure 2.3: Representation of the degree of wetting in terms of the contact angle, θ	9
Figure 2.4: Phase diagram of Cu-Sn	14
Figure 3.1: Outline of the experimental setup for dipping experiments	20
Figure 3.2: Photograph showing the experimental setup for the dipping and reflow experiments	21
Figure 3.3: Temperature-time curve of a typical reflow process at 250°C	23
Figure 3.4: Outline of the experimental setup for reflow experiments	24
Figure 3.5: Optical micrograph showing the IMC layer and its trace	25
Figure 3.6: Micrograph showing reduction in copper thickness during dipping	25
Figure 3.7: Photographs showing a digital planimeter	26
Figure 3.8: Micrograph showing the reduction in copper thickness during reflow	28
Figure 4.1: Micrograph showing various layers in a soldered joint	29
Figure 4.2: Micrographs showing the IMC layer for pure Sn at varying dwell time during **dipping process**	
(a) **Solder:** Pure Sn; **Solder Temp.:** 232 °C	31
(b) **Solder:** Pure Sn; **Solder Temp.:** 250 °C	32
(c) **Solder:** Pure Sn; **Solder Temp.:** 275 °C	33
(d) **Solder:** Pure Sn; **Solder Temp.:** 300 °C	34

Figure Title					Page
Figure 4.3: IMC layer for Sn-Ag at varying dwell time during **dipping process**					
	(a)	**Solder:** Sn-3.5%Ag;	**Solder Temp.:** 221 °C		35
	(b)	**Solder:** Sn-3.5%Ag;	**Solder Temp.:** 250 °C		36
	(c)	**Solder:** Sn-3.5%Ag;	**Solder Temp.:** 275 °C		37
	(d)	**Solder:** Sn-3.5%Ag;	**Solder Temp.:** 300 °C		38
Figure 4.4: Micrographs showing the IMC layer at varying temperatures during **dipping process**					
	(a)	**Solder:** Pure Sn;	**Dipping Time:** 2 min		39
	(b)	**Solder:** Sn-3.5%Ag;	**Dipping Time:** 2 min		40
Figure 4.5: Charts showing average IMC thickness as function of dwell time at different solder temperatures					
	(a)	**Solder:** Pure Sn;	**Process:** Dipping		41
	(b)	**Solder:** Sn-3.5%Ag;	**Process:** Dipping		42
Figure 4.6: Micrographs showing the IMC layer at varying dwell time during **reflow process**					
	(a)	**Solder:** Pure Sn;	**Solder Temp.:** 232 °C		44
	(b)	**Solder:** Pure Sn;	**Solder Temp.:** 250 °C		45
	(c)	**Solder:** Pure Sn;	**Solder Temp.:** 275 °C		46
	(d)	**Solder:** Pure Sn;	**Solder Temp.:** 300 °C		47
Figure 4.7: Micrographs showing the IMC layer at varying dwell time during **reflow process**					
	(a)	**Solder:** Sn-3.5%Ag;	**Solder Temp.:** 221 °C		48
	(b)	**Solder:** Sn-3.5%Ag;	**Solder Temp.:** 250 °C		49
	(c)	**Solder:** Sn-3.5%Ag;	**Solder Temp.:** 275 °C		50
	(d)	**Solder:** Sn-3.5%Ag;	**Solder Temp.:** 300 °C		51
Figure 4.8: Micrographs showing the IMC layer at varying temperatures during **reflow process**					
	(a)	**Solder:** Pure Sn;	**Reflow Time:** 2 min		52
	(b)	**Solder:** Sn-3.5%Ag;	**Reflow Time:** 2 min		53

Figure Title	Page

Figure 4.9: Charts showing average IMC thickness as function of dwell time at different solder temperatures

(a) **Solder:** Pure Sn; **Process:** Reflow 54

(b) **Solder:** Sn-3.5%Ag; **Process:** Reflow 55

Figure 4.10: Micrograph showing the presence of ε and η-phase in IMC 56

Figure 5.1: Reduction in copper thickness as function of dwell time at various solder temperatures

(a) **Solder:** Pure Sn; **Process:** Dipping 60

(b) **Solder:** Sn-3.5%Ag; **Process:** Dipping 61

Figure 5.2: Reduction in copper thickness as function of dwell time at various solder temperatures

(a) **Solder:** Pure Sn; **Process:** Reflow 63

(b) **Solder:** Sn-3.5%Ag; **Process:** Reflow 64

Figure 5.3: Micrographs showing the presence of open channels in IMC in pure Sn. 66

Figure 5.4: Charts showing difference in copper thickness reduction between pure Sn and Sn-Ag during dipping process 67

Figure 5.5: Charts showing difference in copper thickness reduction between pure Sn and Sn-Ag during reflow process 68

Figure 6.1: Arrhenius plot of *D* values for IMC growth during dipping process 72

Figure 6.2: Arrhenius plot of *D* values for IMC growth during reflow process 73

Figure 6.3: Comparison of the Arrhenius plots for IMC growth during reflow process 74

Figure 6.4: Arrhenius plot of *D* values for copper reduction during dipping process 77

Figure 6.5: Arrhenius plot of *D* values for copper reduction during reflow process 78

LIST OF TABLES

Title	Page
Table 2.1: Lead-free solder candidates with typical processing temperatures and features	11
Table 6.1: Estimated values of IMC growth parameters	70
Table 6.2: Estimated values of parameters for copper dissolution	76

CHAPTER - 1

INTRODUCTION

Soldering is one of the oldest techniques of joining two pieces of metals together. Historically, the method dates back to more than two thousand years. In a simple soldering process, the joint gap between the metals to be joined is filled with an alloy called solder, (usually a mixture of two or more pure metals) which has a lower melting point than the joint members. After heating, the solder alloy melts around the members to be joined and upon solidification, forms a permanent bond between them.

At present, soldering technology has become indispensable for the interconnection and packaging of virtually all electronic devices and circuits [9]. The fast changing technology and increasing demands of miniaturization in electronic devices put a challenge before scientists and engineers for obtaining reliable and successful joints of the components. An electronic interconnection is very small in size; for example, a bonding wire is typically of the order of 0.001 inch (25 μm) in diameter [16]. In general a very high density of these interconnections is required on a substrate. The small size of these joints requires high precision in handling to ensure good registration of one joining pad to another pad. In case of a solder interconnection between two copper pads, it is very important to ensure that the pad is not totally dissolved by the tin in the solder. Also, the rate of solidification of the interconnection controls the grain size [16]. Due to these reasons, the science of soldering has extensively been studied in the last several decades.

Traditional tin-lead solders contain a high percentage of lead. Due to environmental and health concerns, alternate lead-free solders are being searched

intensively to replace tin-lead solders. Almost all the potential candidate materials are high Sn containing alloys, including the most promising Sn-Ag alloy at eutectic composition.

During a soldering process, copper is dissolved into solder and reacts with Sn to form an intermetallic compound (IMC) layer at the solder/copper interface. Although the formation of the IMC layer is desirable for good wetting and bonding, an excessively thick layer is harmful because of its brittle nature that makes it prone to mechanical failure even at low loads. Therefore, the control of copper dissolution during soldering and resulting thickness of the IMC layer is of particular importance to the integrity of the joint and thus to the reliability of the electronic devices.

The copper dissolution rate and resultant growth of IMC layer in soldering reaction has been a critical issue in the electronic packaging industry. The growth rate of the IMC layer is determined both by temperature of the solder and dwell time (time for which the molten solder remained in contact with the substrate).

1.1 Objective of the Study

In the present study, the dissolution of copper and growth of Cu-Sn intermetallic compound at the solder/copper interface is investigated. The phenomenon is analyzed as a function of dwell time and temperature of the molten solder for two different solders, the pure Sn and Sn-3.5wt%Ag. Growth kinetics of copper dissolution and development of IMC for the two solders during dipping and reflow process will also be investigated. Kinetics parameters will be calculated for dissolution of copper and growth of IMC in the two processes.

CHAPTER - 2

LITERATURE REVIEW

2.1 Soldering Process

There are numerous soldering techniques employed in the electronic packaging industry. These techniques are specific to particular need and application. Variations in soldering methods arise due to different schemes in applying heat, flux and solder material to the joining components. However, all the soldering techniques can broadly be categorized into two basic methods viz. reflow soldering and wave soldering. Currently, these methods are predominantly used by the electronic packaging industry.

2.1.1 Reflow Soldering

In reflow soldering, a mixture of solder and flux called the solder paste is applied to every joint to be made in the assembly. Heat is applied by means of radiation, conduction or convection in a controlled environment. The whole assembly is heated up and held at some temperature followed by cooling. During the process the solder melts and fills the gaps around, forming the joint. An added benefit of this approach of soldering components to the printed circuit boards and cards is that there is no geometry dependence, nor is there any limitation to types of components on a board such as surface mount. The operational sequence of a reflow soldering process is:

1. Apply the solder paste (solder and flux) to the joint
2. Apply heat
3. Cooling to the room temperature

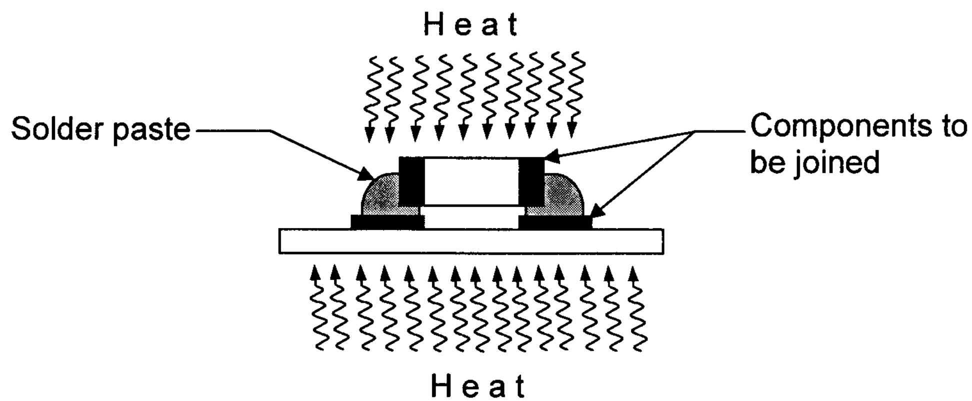

Figure 2.1: Schematic diagram showing the principle of reflow soldering

2.1.2 Wave soldering

In wave soldering, the printed circuit board populated with the components to be joined is passed across the crest of a molten, standing solder wave. Only the bottom of the board is exposed to the molten solder. The molten solder serves both as the source of heat to the board and components, as well as the solder source for the joints. The operational sequence of a wave soldering machine is:

1. Applying the flux
2. Applying heat
3. Applying solder and heat
4. Cooling to the room temperature

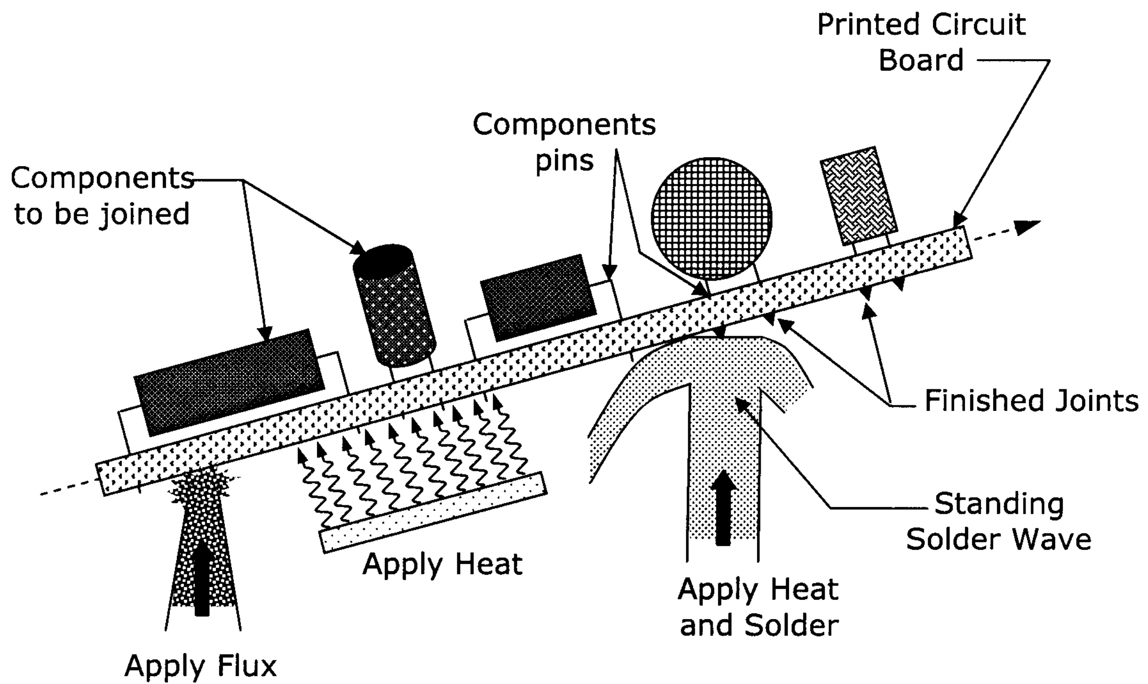

Figure 2.2: Schematic diagram showing the sequence of wave soldering

2.2 Solder Materials

Solder joints are not merely the electric interconnections between the components but they also serve as the mechanical support and heat dissipater for the device. Choice of solder is a very important factor and critical both to the soldering process and reliability of the joint during service.

The quality of soldered joints depends strongly on the combination of filler and component materials, including the processing conditions. It is for this reason that a sound understanding of the metallurgical changes accompanying the sequence of events

that occurs in making soldered joint is so vital for the development of a reliable joint. Theoretical principles have helped to furnish insights, guidelines and qualitative explanation for the soldering technology, but have rarely provided reliable data for use in the design of joining processes. In reality the soldering process is extremely complex, because it brings into play a large number of variables, some of which may not be easy to recognize and understand. Among the relevant factors are the condition of the solid surfaces (i.e. nature of other coatings, oxides, sulfides, surface roughness etc.), the temperature gradient that develops during the joining operation, the metallurgical reaction involving the filler and parent material, and the chemical reactions with fluxes if they are used [14].

The traditional tin-lead solder has a long history in soldering process. This solder and the alloys developed with it provide many benefits such as ease of handling, low melting temperature, good workability, ductility and excellent wetting on copper and its alloys [9]. Lead bearing solders, and especially the eutectic or near-eutectic Sn-Pb alloys, have been used extensively in the assembly of modern electronic circuits. [9].

Although, several commercial and experimental Sn-based, lead free solder alloys exist, none meets the standards, which include the required material properties such as low melting temperature, wettability, mechanical integrity, good manufacturability, and affordable cost. Current processing conditions and equipment (involving fluxes) are optimized for Sn-Pb solder alloys over the past 30 years. The development of proper assembly processes for lead-free solders is also needed [9].

A number of alloy systems are available to serve as solders for industrial use. Each alloy is unique with regard to its properties and must be chosen to meet the

requirements of the assembly, such as ductility, resistance to low-cycle fatigue, tensile and shear strength, and rate of consumption of the base metal in solder and/or substrate [16].

2.2.1 Factors Governing the Choice of Solder

2.2.1.1 Environmental Concern

Increasing environmental and health concerns related to the toxicity of traditional tin-lead solders and the legislations that limit the usage of lead bearing solders, have provided the much desired impetus for intensive research efforts at developing alternate lead-free solders [6,9]. The first step in finding suitable alloy candidates is, therefore, to search for some nontoxic, low melting temperature alloys which can replace the Pb [9].

Almost all the potential candidate materials, to include the promising Sn-Ag alloy of eutectic composition, are high-tin alloys [6]. The candidate alloy components involve Sn as the base element, Ag, Bi, Cu, and Zn as the major alloying elements, and some other minor additions such as In and Sb. Among these elements In is known to be the precious metal with limited world production. Given its scarcity, In cannot become a major alloying element [9].

Conventional tin-lead solders are prone to inferior fatigue properties during thermal excursions and/or cycling. A harder alloy with high melting point and enhanced mechanical properties is needed to obtain durable solder joints [4]. The Sn-(3-3.9)%Ag alloy offers improved mechanical properties and good interfacial bonding [9].

2.2.1.2 Process Conditions

The current processing equipment and conditions for electronic assembly are optimized for Sn-Pb solders. Any new conditions for lead-free alloys must ensure both productivity and reliability at least equivalent to present level of Sn-Pb solders. One of the most sensitive parameter for the quality of soldered joints is soldering temperature. The melting temperature of Sn-Pb eutectic alloy is 183°C, and the typical soldering temperatures are 230°C and 250°C for reflow and wave soldering respectively. The temperature margin beyond the melting temperature of the solder is about 50°C for reflow soldering. In contrast, melting temperature for typical lead-free solders are higher than Sn-Pb eutectic solders by about 30°C, which makes the process window narrower. Because some of the electronic components cannot at present withstand an increase in reflow temperature, processing conditions need to be developed to incorporate heat-resistant components [9].

2.2.1.3 Wetting

Wetting is very important for solders because reliable interconnection requires good wetting. Good wetting results in well formed solder fillets. The liquid solder is sometimes constrained from spreading away by surrounding the surface around the confines of the joint with a nonwettable material (a solder mask). The ability of liquid to wet a solid surface is measured in terms of the contact angle. The contact angle is the angle that the liquid solder makes with the solid base metal surface. Figure-3 illustrates the relationship between the dihedral angle, θ and the degree of wetting. A contact angle of less than 90 degrees indicates lack of wetting affinity. To ensure good wetting, the

molten solder should wet the connecting surface with a contact angle of less than 10 degrees [16].

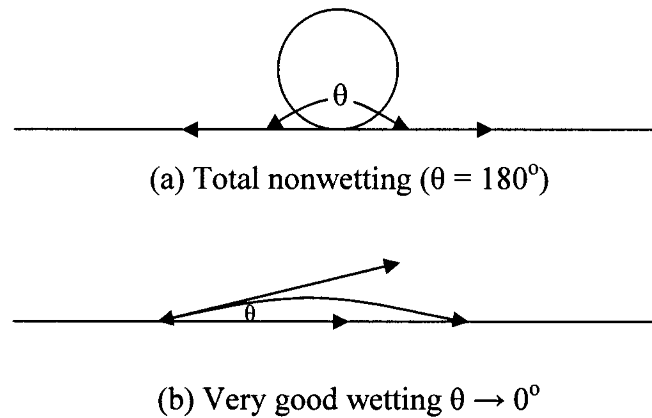

Figure 2.3: Representation of the degree of wetting in terms of the contact angle, θ

Most lead-free solders seem to exhibit poorer wetting on Cu than Sn-Pb near eutectic alloy solders. It is well known that small amounts of certain impurities in the solder alloy influence the mechanical properties of an interconnection, and the degree of wetting of the molten solder [16]. Addition of Ag slightly promotes wetting on Cu. However, addition of Bi improves wetting significantly. Improved fluxes have also enhanced wetting behavior of solders [9,14].

2.2.1.4 Reliability and Cost

Reliability in electronic soldering involves various factors: strength, ductility, thermal and mechanical fatigue, creep, and shock resistance. Since most of the solders have low melting temperature, it is difficult to understand the various behaviors around room and service temperature. Due to the reason that diffusion of elements is quite active

and creep can occur even at room temperature, the reliability of the soldered joints is a critical issue [9].

Cost is another important factor in selecting a solder for practical electronic application. In general, taking cost of raw metals into consideration, most lead-free solders cost about two to three times more than Sn-Pb solders. In contrast, the cost of Sn-0.7wt%Cu eutectic solder is only about 1.3 times higher than Sn-Pb solder, which explains why Sn-Cu has been successfully transferred to practical production of consumer products. Table 1 summarizes the candidate lead-free solder alloys with their respective features [9].

Table 2.1: – Lead-free solder candidates with typical processing temperature and features* [9]

Candidates	Temperature (°C)		Benefits	Drawbacks
	Wave Soldering	Reflow Soldering		
Sn-(3-3.9)% Ag [(0.5-0.7)%Cu] or [(1-3)% Bi]	250-260	235-250	Excellent Mechanical properties Soldering temperature can be lowered by Bi	High soldering temperature Lift off** with Bi and Pb Partial melting reaction at 139° C with much Bi Poor compatibility with various alloys and Sn-Pb plating
Sn-57% Bi [(0.5-1.0)% Ag]		180-200	Low soldering temperature	Very brittle but can be improved by adding Ag Poor heat resistance
Sn-(8-9)% Zn [3% Bi]	~250	220-230	Same soldering temperature as for eutectic Sn-Pb	Severe oxidation but can be improved by flux Poor heat resistance of interface with Cu
Sn-0.7% Cu [Ag, Ni, Au]	250-260		Cheaper cost	High soldering temperature Lift-off** with Pb

*Figures in [] are the third alloying elements and their typical compositions
**Lift-off is type of failure when upon cooling from soldering; the fillet is peeled from a Cu land located on a printed circuit board.

2.3 Soldered Joints

Soldering is based on a surface reaction between the metal, which is to be soldered (the substrate) and the molten solder. This reaction at the interface is of fundamental importance because if this reaction does not occur, there will be no bonding between the solder and the substrate and consequently a joint will not be formed. The control of the interface reaction is crucial for both the process of soldering and the reliability of the resulting soldered joint. The reaction products, also called the intermetallic compounds, are formed at the interface of the solid substrate and the molten solder. The formation and growth of the intermetallic layer has a profound effect on the mechanical properties of the joint and its behavior during its service life [14].

Any non-metallic surface layer, such as an oxide or sulfide on the substrate or the solder prevents the soldering reaction at the interface. Flux is added to remove the layer and prevent it from forming during soldering. It is important to note that the flux only facilitates in the reaction to take place but it does not take part in the interface reaction [16].

2.3.1 Intermetallic Compound Layer

During a soldering process, copper dissolves in the molten solder and reacts with tin. As a result a layer of the intermetallic compound is formed at the interface of the solid substrate and the molten solder. Intermetallic phases produced by soldering in electronic packaging are stoichiometric binary compounds containing Sn. The most common intermetallic compounds formed during soldering are from the Cu-Sn, Au-Sn, Ni-Sn binary systems [16]. Elemental Pb or Bi does not react with the commonly used

base metals like Cu, Au, Ni or Pd. Thus, in Sn-Ag, Sn-Pb or Sn-Bi solders, only Sn will react with the base material (most often Cu) to form an intermetallic phase [16]. The occurrence of Cu-Sn phase upon soldering becomes apparent when viewing the Cu-Sn phase diagram (Figure - 4), which reveals the presence of two stoichiometric compounds corresponding to the compositions of Cu_3Sn and Cu_6Sn_5 [16]. The phase near the copper substrate has been observed to be Cu_3Sn and is normally termed as ε-phase, while the one next to it is observed to be Cu_6Sn_5 and is termed as η phase [12]. X-ray diffraction was used to identify these phases by Lee and Duh [13]. Compositions of IMC layer were further quantitatively measured. The molar ratio of the Cu/Sn was about 6:5, which is close to stoichiometric composition of Cu_6Sn_5 in the metallic layer near the solder side. In the intermetallic layer near the copper side, the molar ratio of Cu/Sn is around 3:1, approaching the stoichiometric composition of Cu_3Sn [13].

The thickness of IMC depends on several factors. Of them the composition of solder material, maximum temperature reached during soldering and the length of time during which the substrate was exposed to the molten solder (dwell time) are most important. IMC growth is favored both by the increase in soldering temperature and dwell time. The maximum soldering temperature reached and the dwell time vary widely between different soldering methods. The IMC thickness is profoundly affected by the soldering temperature and dwell time [14]. Another important factor governing the final thickness and quality of the intermetallic compound is the rate at which the solder joint is cooled. It has been observed that faster the rate of solidification, lesser the growth of the intermetallic layer and finer the grain structure of solder in the joint.

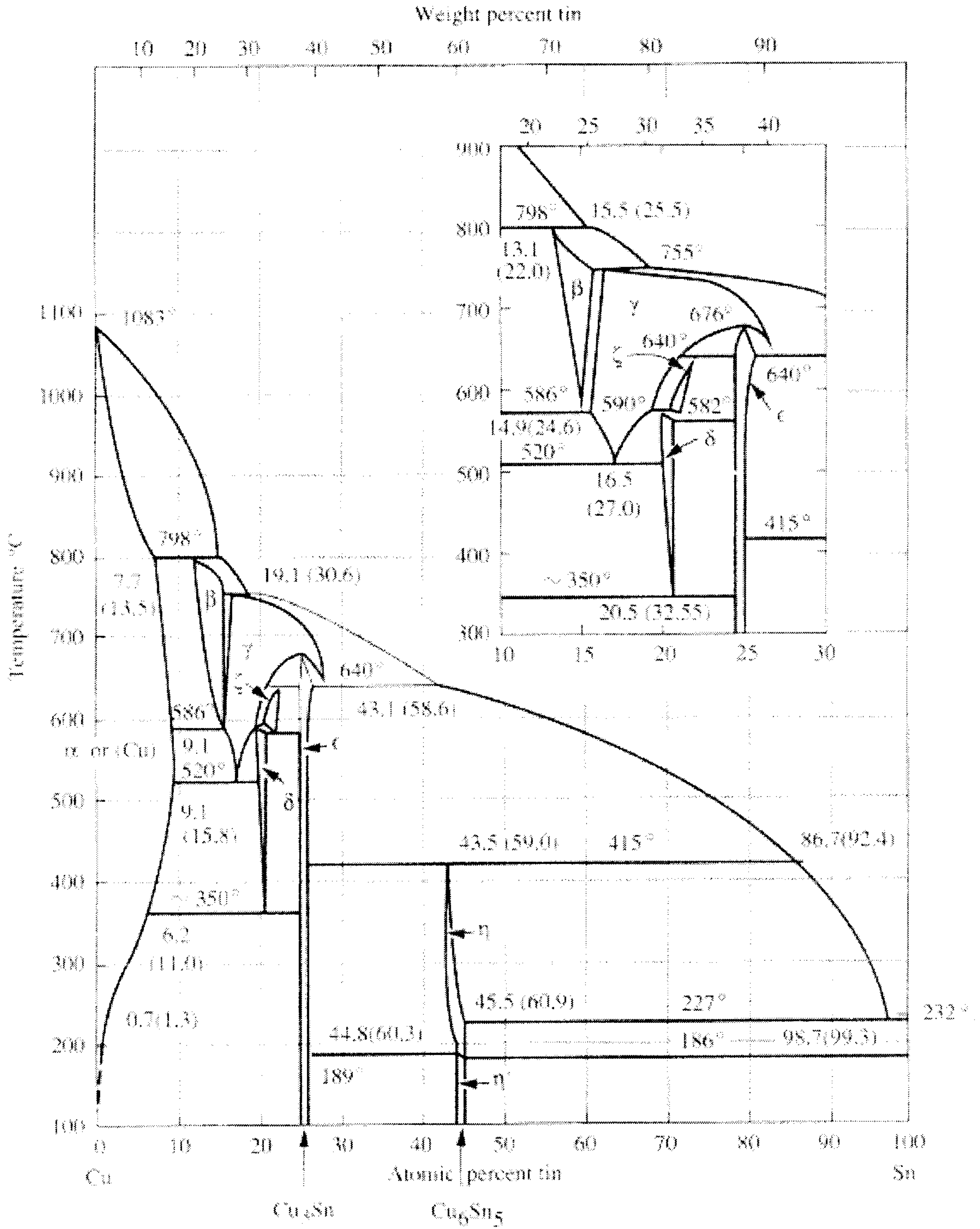

Figure 2.4: Phase diagram of Cu-Sn [16]

Although formation and presence of the intermetallic compound layer is desirable for good wetting and bonding, an excessively thick layer is detrimental due to its intrinsic brittleness which makes it prone to mechanical failures even at low loads [12]. The brittle nature of an intermetallic phase is in part a result of the ordered crystal structure of the compound phase [16]. Also, an excessively thick intermetallic compound layer results in a joint having non-uniform physical and electrical properties, like coefficient of thermal expansion and elasticity [9]. The solderability of pretinned circuit boards may be degraded by the intermetallic compound penetrating the pretinned surface and deteriorating its wettability in subsequent soldering operations [14,15].

Uncontrolled growth of IMC poses the weakness in the soldered joint and causes microstrains due to the mismatch of the thermal expansion coefficient between the solder and IMC [7]. As the microstrains exceed a critical value, microcracks occur at the interface of solder/IMC and might propagate, which would result in failure of the joint and hence influence the reliability of solder joints [7]. Further, the film could continue to grow during service if the joint attains high temperatures due to internal heat generated by the chip or heat dissipated from external environment [12]. The growth of IMC in the solid state is thought to depend, to some extent, on the initial film that formed during reflow process [12]. It is argued that the degradation of the solder joint is related to the thickness of IMC and to the kinetics of IMC growth during soldering [7]. In order to prevent the excessive growth of thick intermetallic layers, a barrier layer is often deposited on the copper base metal contacting the molten solder alloy. Nickel is most often used as a barrier layer between solder and copper. Ni reacts with the Sn to produce Ni-Sn intermetallic phases, which grow much more slowly than Cu-Sn intermetallic phases at high temperatures [16].

2.3.1.1 Morphology of Intermetallic Layer

A core issue in soldering is the formation of intermetallic compounds between the solder and the substrate. In solid-state aging planar layer growth is typical for the interfacial intermetallic formation [21]. However in liquid-state soldering, the scalloped growth is dominant, which is accompanied by a ripening process [1,6,20,21]. While the temperature difference between these two reactions is less than 100°C, the resultant intermetallic interfacial morphologies differ dramatically [20]. It has been suggested that a non-conservative ripening process contributes to the scalloped structure formation, resulting in coarsening of the scallops that decrease in number with time [5,6,20]. In ripening process, due to the Gibbs-Thomson effect, the smaller intermetallic grains dissolve into the liquid solder, feeding to further growth of their neighboring larger grains. Therefore, the dissolution of the intermetallic compound plays a key role in the intermetallic growth [5]. The dissolution kinetics may be the limiting factor for the ripening process if the dissolution rate (the rate of decomposition of intermetallic compound into its component atoms) is smaller than (or comparable with) the solute diffusion rate in the liquid solder. This may happen during high temperature soldering when the diffusivity of solute is relatively high [5].

It has also been reported that the dissolution of the intermetallic compound reduces the average thickness of the intermetallic layer during reflow [1,22].

2.3.2 Dissolution of Copper

During a soldering process, copper dissolves into molten solder. Dissolution of copper in lead-free solders is observed to be much higher than in lead-based solders,

since in the lead-containing solders there is more tin available to form the Sn-Cu compound [8]. In addition, reaction between the high tin-containing solder and copper is intense during soldering, which favors quick depletion of copper. Rapid depletion of copper is conducive for dewetting and failure of the joint. As the thickness of copper is limited and the rework and/or repair of a solder joint requires a layer of unreacted copper, the loss of copper during soldering process must be kept under control [6]. Therefore, the dissolution of copper at the solder/copper interface is of particular importance to the integrity of soldered joints and the overall reliability of electronic devices [2].

The dissolution and reaction depends upon the relative amounts of solder and substrate material. When there is a small amount of solder available compared to the substrate, the solder saturates quickly, after which dissolution decreases and fast intermetallic growth can occur. On the other hand, if there is a large amount of solder available, dissolution dominates and resulting IMC thickness is low [8].

2.4 Kinetics of Copper Dissolution and IMC Growth

The kinetics of copper dissolution and growth of IMC can be quantified based on thickness measurements. Dissolution of the substrate and resulting growth of intermetallic compounds both follow Arrhenius-type rate relationships, represented by the expression in equation (1) [1,2,15]

$$x(T,\ t) = Dt^n \tag{1}$$

where:

x is the thickness of the IMC layer

t is the dwell time

T is the temperature of molten solder

D is the diffusion coefficient, and

n is a constant

The diffusion coefficient D is related to temperature through the Arrhenius equation:

$$D = D_o \exp(-Q / RT) \quad (2)$$

where:

D_0 is a pre-exponential temperature-independent constant

Q is the activation energy of the solute (copper in this case), and

R is the universal gas constant

The activation energy for diffusion, Q, to a first approximation, is proportional to the melting point of the particular metal [15]. The rate-controlling step for reaction between two solid metals is the diffusion of atoms between the reacting phases [15]. In general, the concentration of dissolved metal in the molten filler increases in an inverse exponential manner with respect to time. That is, the dissolution rate is initially very fast, but then slows as the concentration of the dissolved parent material tends toward its saturation limit (i.e. equilibrium) [15].

In some materials systems, the product of reaction between molten filler and the parent materials is a continuous layer of an intermetallic compound over the joint interface. Once formed, the rate of erosion greatly decreases, because it is then governed by the rate of at which atoms of the parent material can diffuse through the solder intermetallic compound [15].

CHAPTER - 3

EXPERIMENTAL PROCEDURES

3.1 Materials and Soldering Procedure

3.1.1 Dipping Experiments

In one series of experiments, around 400 grams each of Sn-3.5 wt %Ag and pure Sn solders were taken and melted separately in a stainless steel crucible. The molten solders were then transferred to 200 ml glass beakers for the two different experiments. Copper samples of size 10 mm × 20 mm × 0.4 mm were cut from a 99.9 % pure copper sheet. The sample substrates were mechanically ground and then finish polished to remove any oxide layer on the surface and to enhance the wettability. The samples were then rinsed in water and alcohol.

Glass containers having molten solders were put in an enclosed furnace maintained at the desired experiment temperature. The temperature of the solder was monitored by immersing a fine gauge chromel alumel thermocouple in the middle of the solder bath. Solder bath temperature was maintained in a close range of ±2 °C of the experiment temperature. The molten solder was maintained at temperatures of 221 °C, 250 °C, 275 °C and 300 °C for Sn-3.5 wt %Ag solder, and 232 °C, 250 °C, 275 °C and 300 °C for pure tin.

A thin coating of mildly activated rosin (RMA) flux was applied to the polished samples. The samples were then dipped vertically in the solder bath. The samples were taken out of the solder vertically at different time intervals ranging from 5 seconds to 10 minutes.

The samples were cut along the length and perpendicular to the solder copper interface using a diamond-cutting wheel. All samples were cleaned with methanol to remove any dirt and/or grease prior to cold mounting in epoxy at room temperature. The mounted samples were then wet-ground using 320, 600, 800 and 1200 grit SiC impregnated emery paper. After grinding, the samples were fine polished using 5 micron, 1 micron and 0.05 micron alumina based lubricant (aluminum oxide suspended in distilled water). The polished samples were then etched for around 1 to 2 seconds using an etchant (a solution mixture of 5 ml HNO_3, 2 ml HCl and 93 ml Methanol).

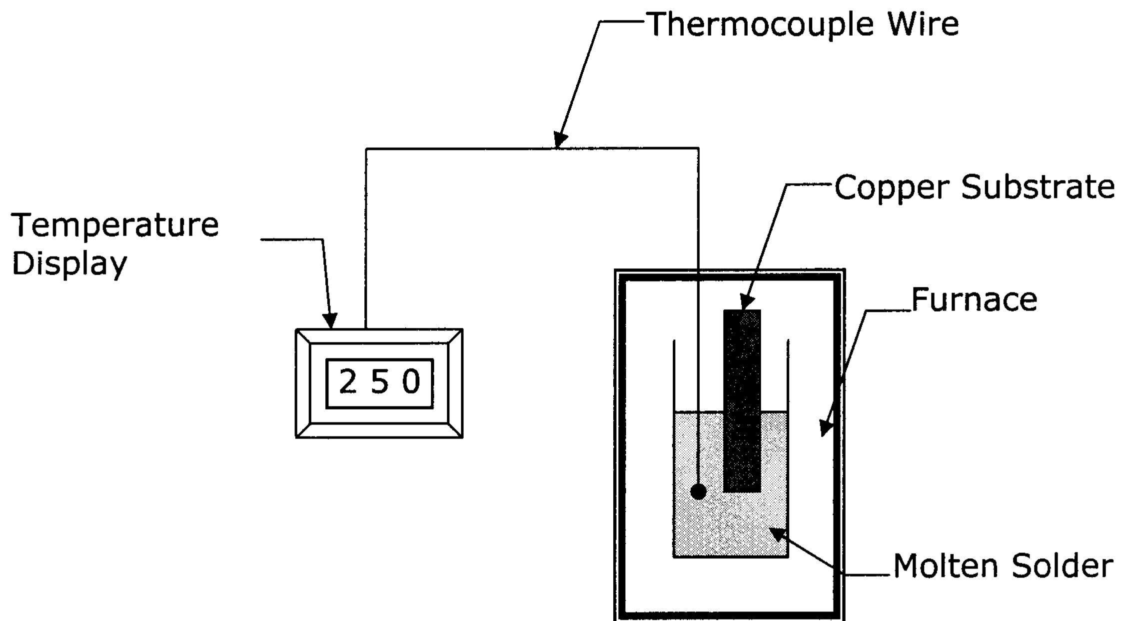

Figure 3.1: Outline of the experimental setup for dipping experiments

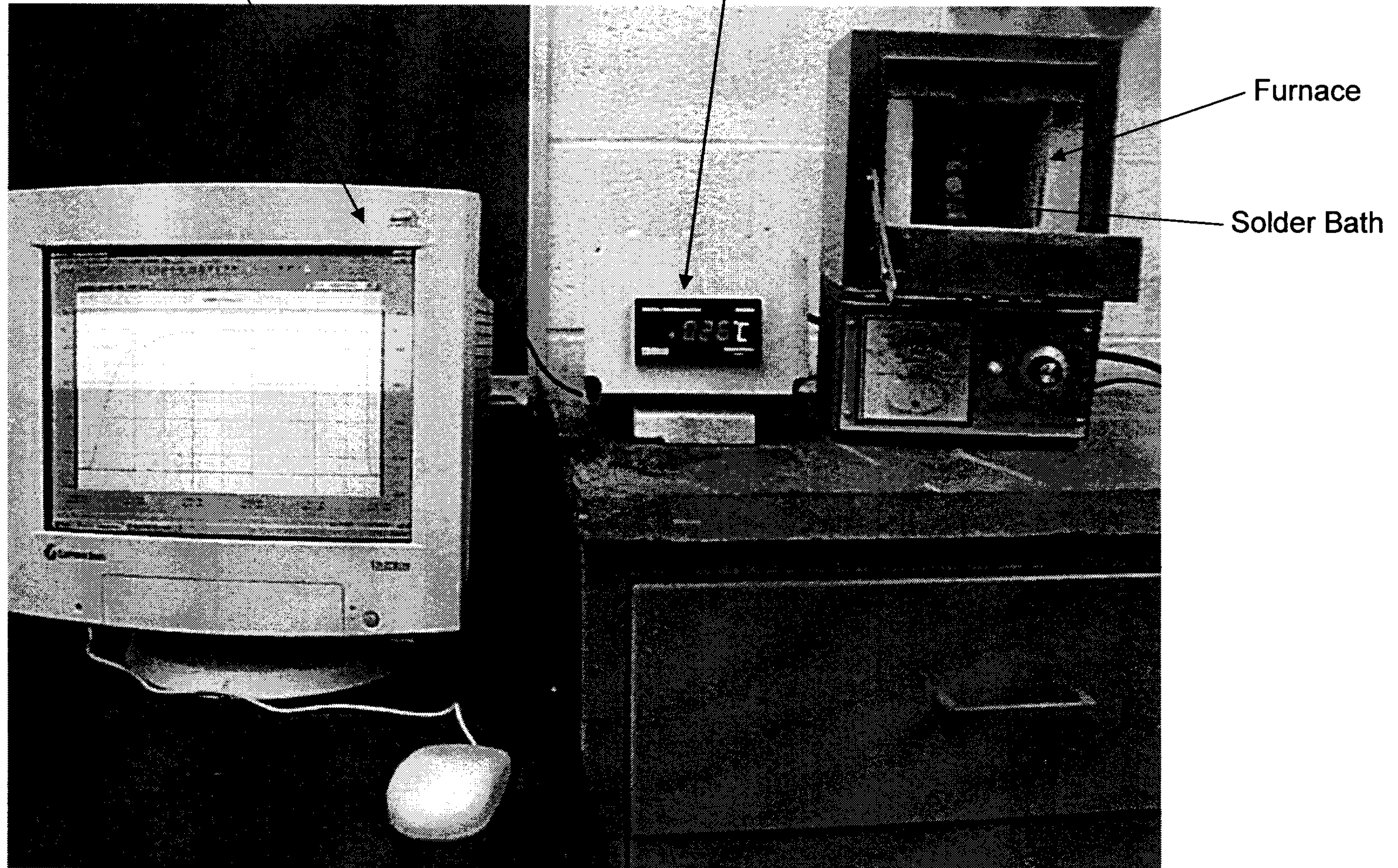

Figure 3.2: Photograph showing the experimental setup for the dipping and reflow experiments.

3.1.2 Reflow Experiments

In other series of experiments, copper substrates were light ground and micro-polished to remove any layer of oxide and improve wettability. The substrate samples were then rinsed with water and alcohol. Solder paste of two different compositions pure Sn and Sn-3.5 wt %Ag was prepared separately by mixing the solder powder in RMA flux. Two solder balls each around 100 mg. of same solder paste were dispensed over the copper substrate. A fine gauge chromel-alumel thermocouple was embedded in one of these balls, which acted as a dummy sample. The dummy sample was used to record the temperature-time profile of the solder copper assembly during soldering. A closed furnace was maintained at the desired experiment temperature. The furnace temperature was monitored with another dummy sample of solder copper assembly embedded with a fine gauge chromel-alumel thermocouple. Copper samples with two solder balls were put in the furnace and the temperature of the assembly was monitored in real time on computer with the help of a data acquisition system. The start of the reflow time was calculated from the time when all solder attained the melting temperature and was in liquid state (Figure 6). The samples were taken out of the furnace after time periods ranging from 10 seconds to 10 minuets and immediately quenched in cold water. The experiments were repeated using different solder compositions and various furnace temperatures; at the melting points of the solders (221 ^{o}C for pure Sn and 232 ^{o}C for Sn-3.5 wt %Ag), 250 ^{o}C, 275 ^{o}C and 300 ^{o}C.

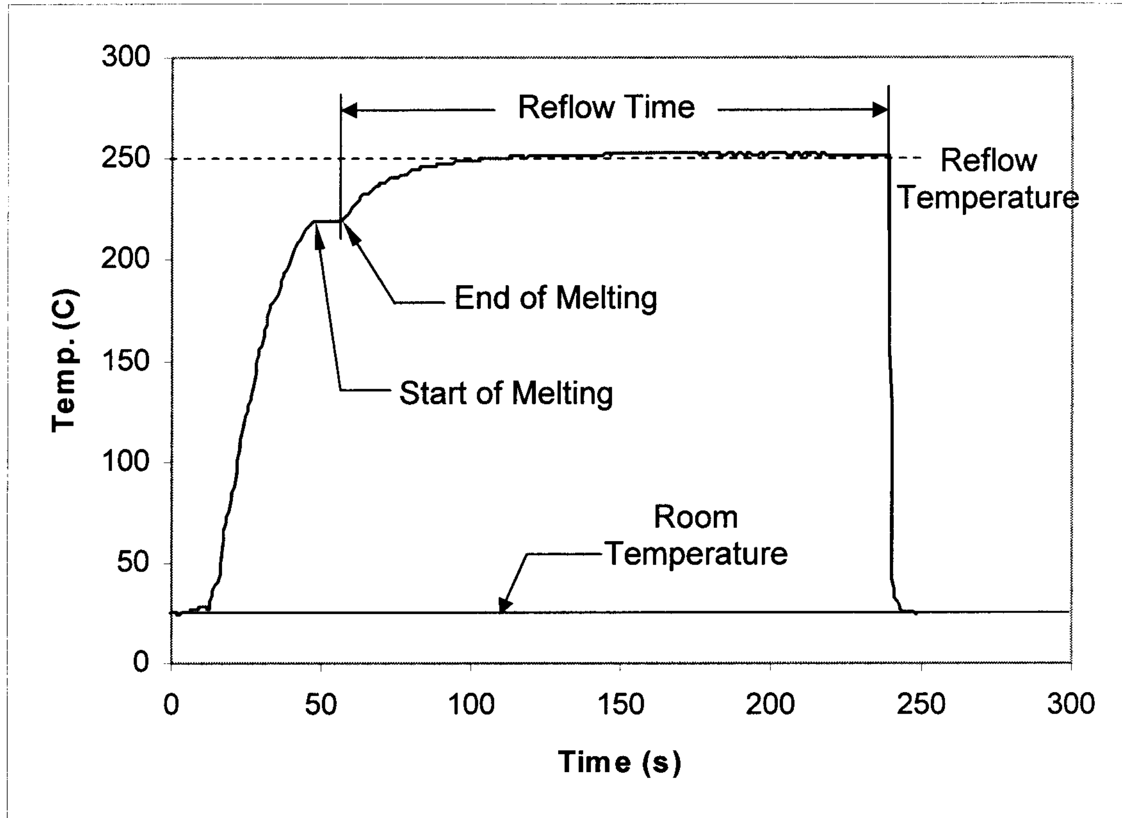

Figure 3.3: Temperature-time curve of a typical reflow process at 250°C.

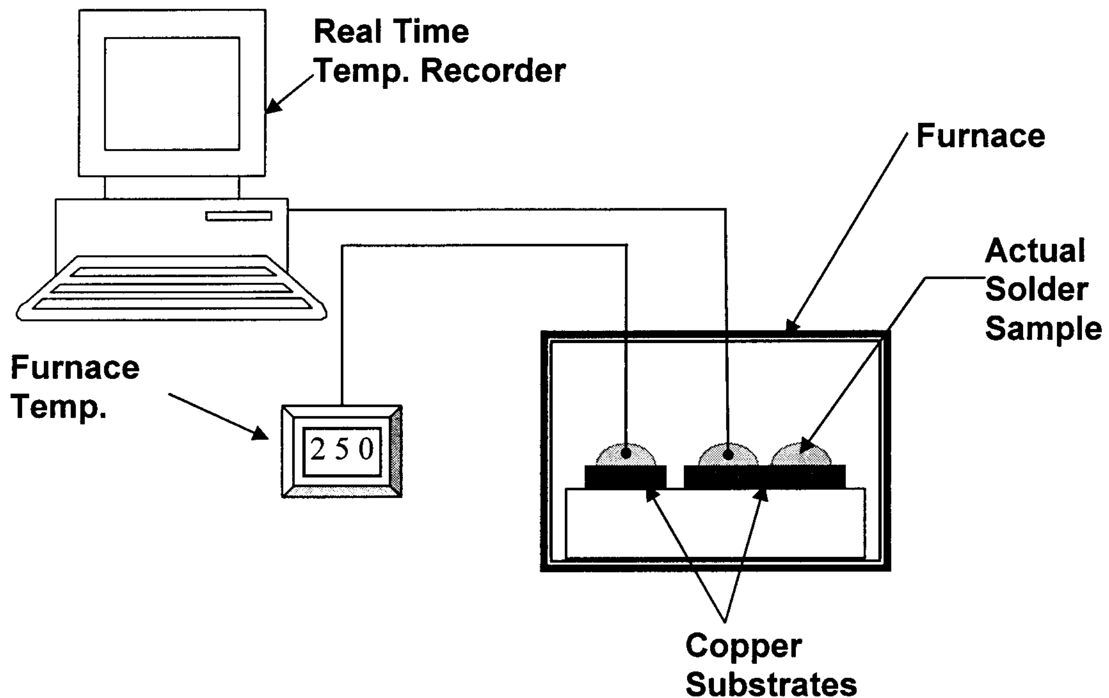

Figure 3.4: Outline of the experimental setup for reflow experiments

3.2 Metallography

The polished and etched samples were examined in a light optical microscope to analyze the formation, presence and growth of the intermetallic compound. The images at the solder copper interface were captured with a digital camera attached to the microscope and stored on a computer. Several images were taken at various sections near the middle of the samples. To calculate the average thickness both in case of dipping and reflow process, the area of IMC, in each micrograph, was manually traced out using a high accuracy digital planimeter (Figure 11). Measurements were repeated three times at each location. Four or five locations were measured for each micrograph. A thin layer of

Cu_3Sn was observed in case of reflow experiments at higher temperatures and longer dwell time. Since the thickness of the layer was very low (≤ 1 micron), it was included in the total IMC thickness of the micrograph.

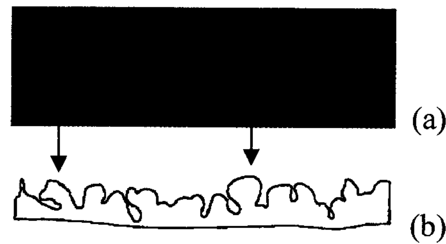

Figure 3.5: Optical micrograph showing the IMC layer (a) and its trace (b) used for the measurement of average thickness by a digital planimeter

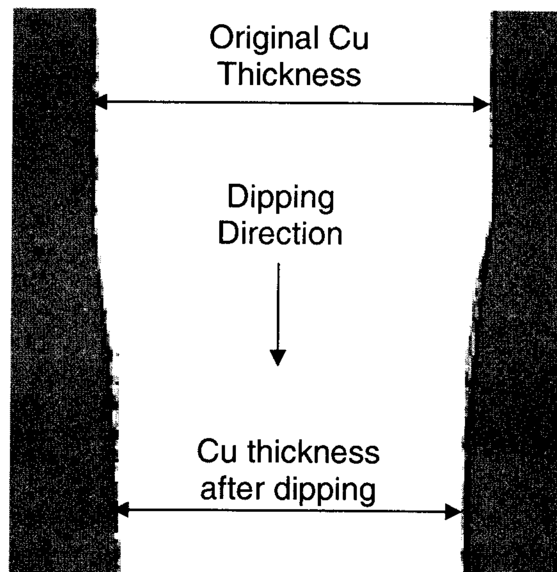

Figure 3.6: Micrograph showing thickness reduction in the copper substrate when dipped in molten solder

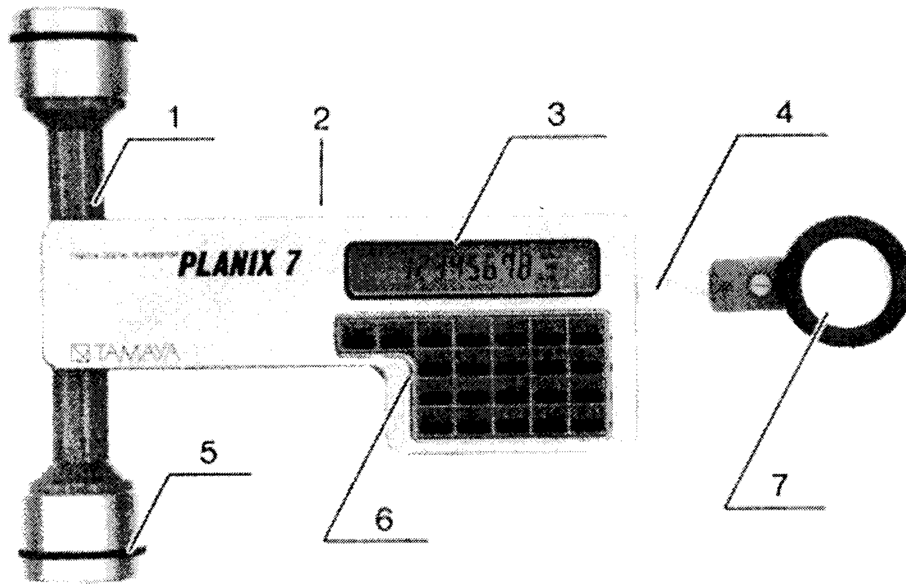

Front

Side

1. Roller Axle
2. Plug
3. Display
4. Tracer Arm
5. Roller
6. Operation Keys
7. Tracer Lens

Figure 3.7: Photograph showing a digital planimeter

To calculate the total copper dissolution in the solder during soldering, it was assumed that a reduction in the thickness of the copper substrate is a good measure and directly proportional to total copper dissolution. For the dipping experiments, the reduced thickness of the copper substrate (Figure 10) was measured at three different locations of each sample, namely: top, middle and bottom. Their average was subtracted from the original thickness (Figure 10) of the sample to get the reduction in total thickness. It is noted that in this experiment, the solder tends to attack the substrate from both sides. Consequently, the measured value of decrease in thickness is twice the value in an actual soldering process, and therefore, only half of the measured value is plotted.

To estimate the dissolution of copper during reflow process, images were taken at the junction of the solder cap and the copper substrate as shown in Figure 12. The images were taken at the right and left ends of the cap. The dissolution of copper was measured as the depth to which the copper solder interface reduced after soldering and then multiplying by the magnification factor of the microscope.

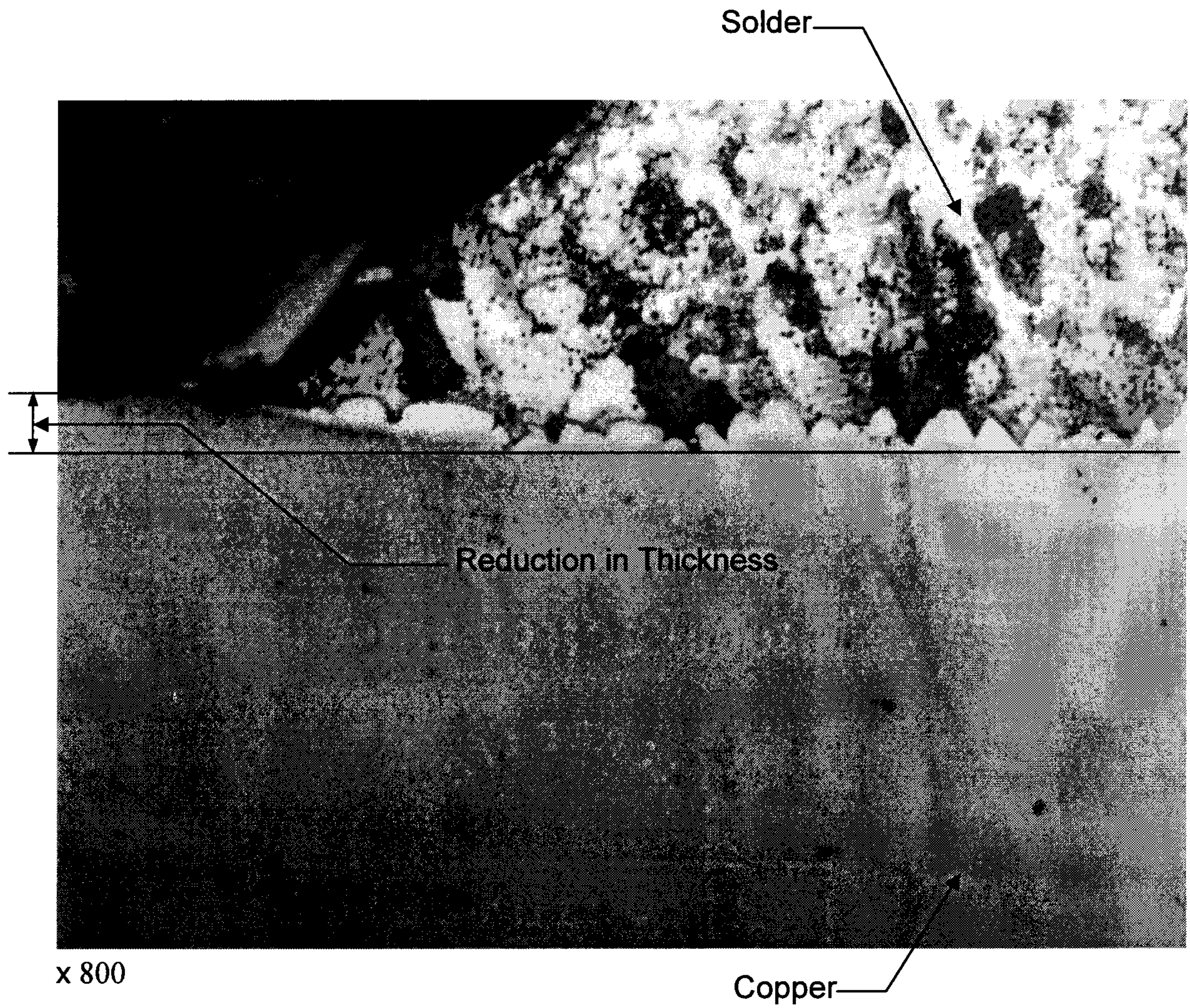

Figure 3.8: Micrograph showing the reduction in copper thickness as result of copper dissolution during reflow soldering

CHAPTER - 4

ANALYSIS OF OBSERVED IMC GROWTH

Growth of the intermetallic compound layer at the solder/copper interface was investigated. Figure 4.1 shows typical optical photograph of the IMC layer. In this photograph, the bottom part is the copper substrate and the top part is the solder. The middle light colored region is the IMC layer. It was observed that the IMC layer did not grow as a regular layered structure. Rather, the IMC phase grows as scallop like grains within the molten solder.

Figure 4.1: Micrograph showing different layers in a solder joint

4.1 Dipping Process

Figures 4.2 show the growth of IMC for pure Sn during dipping process. Similar micrographs for Sn-3.5% Ag solder are shown in Figures 4.3 for dipping at various solder temperatures. The corresponding dwell time and the resultant average IMC layer thickness are also given for each photograph. It was observed that, at a given solder temperature, the thickness of the IMC layer for the two solders was a strong function of dwell time. The average IMC layer thickness increased with increasing dwell time.

The solder material has an important influence on both thickness of the IMC layer and interface morphology. Examination of the micrographs (Figure 4.2 and 4.3) revealed

that the Sn-Ag alloy can result in a thicker intermetallic compound layer except for a short dwell time (5 seconds). This observation indicates that the addition of silver can favor intermetallic compound growth.

Another important parameter controlling the growth of the intermetallic compound layer is the temperature of the molten solder. Figure 4.4 (a) and (b) show the end IMC layer thickness and structure for both pure Sn and Sn-3.5%Ag solders during dipping process at different temperatures and for the same dwell time. It is evident from the micrographs that a higher solder temperature yield greater IMC thickness, as expected.

The evolution of thickness of the intermetallic compound layer for dipping process, as function of the dwell time at different temperature, is shown in Figure 4.5 (a) and (b). It is evident from the curves that IMC growth is a strong function of dwell time and temperature of the solder. The average intermetallic compound layer thickness increased with dwell time and solder temperature. The IMC growth rate at all temperatures is high during the initial stage and then gradually slows down during the terminal stages. The recorded initial high growth rate of the intermetallic compound layer is attributed to the diffusion of tin along grain boundaries of the fine IMC grains formed at the beginning of IMC layer growth. As the IMC grains thickened and concurrently coarsened, diffusion of tin to the copper substrate became difficult, and consequently, resulted in an actual decrease in intermetallic compound growth rate.

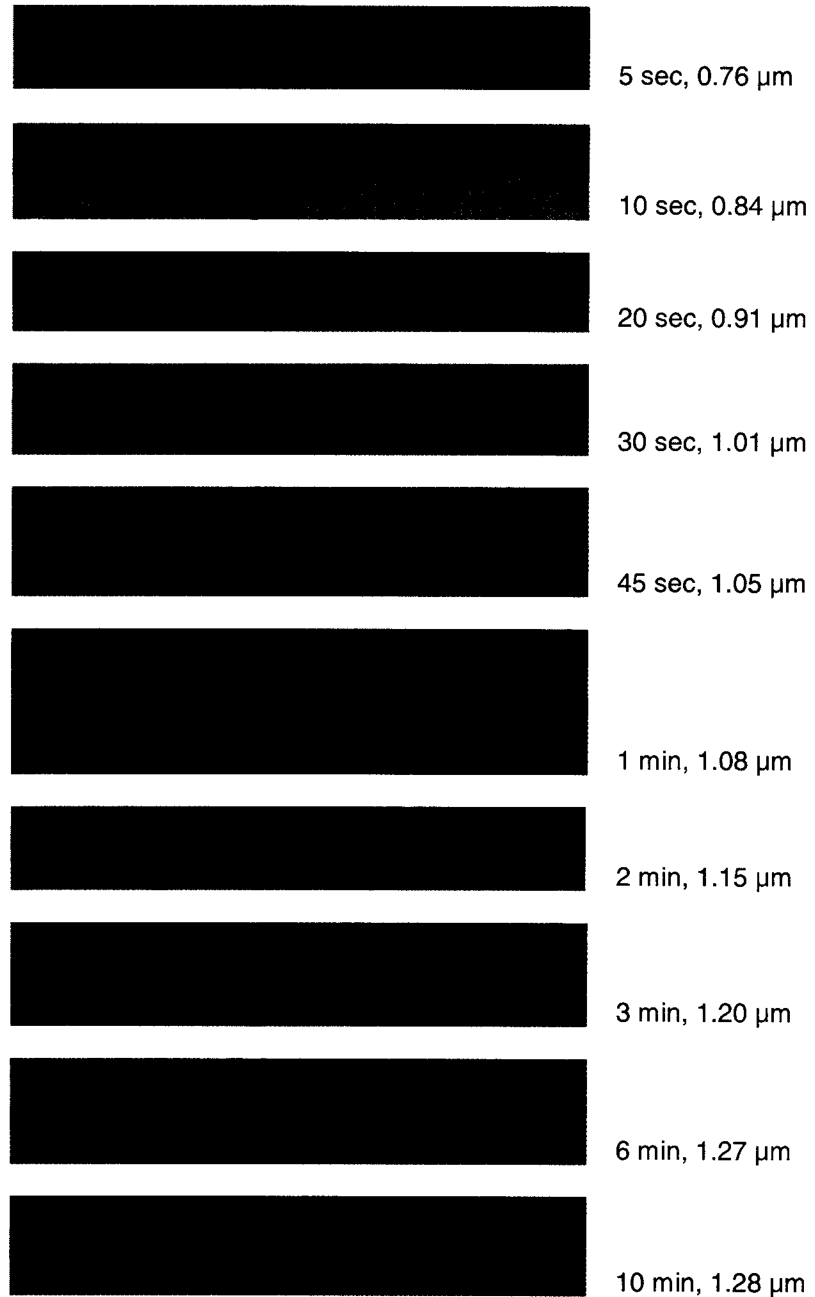

Process	Dipping
Solder:	Pure Sn
Solder Temp.:	232 °C

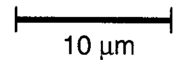

Figure 4.2 (a): Micrographs showing the IMC layer at varying dwell time. The dwell time and average IMC thickness is written by each micrograph

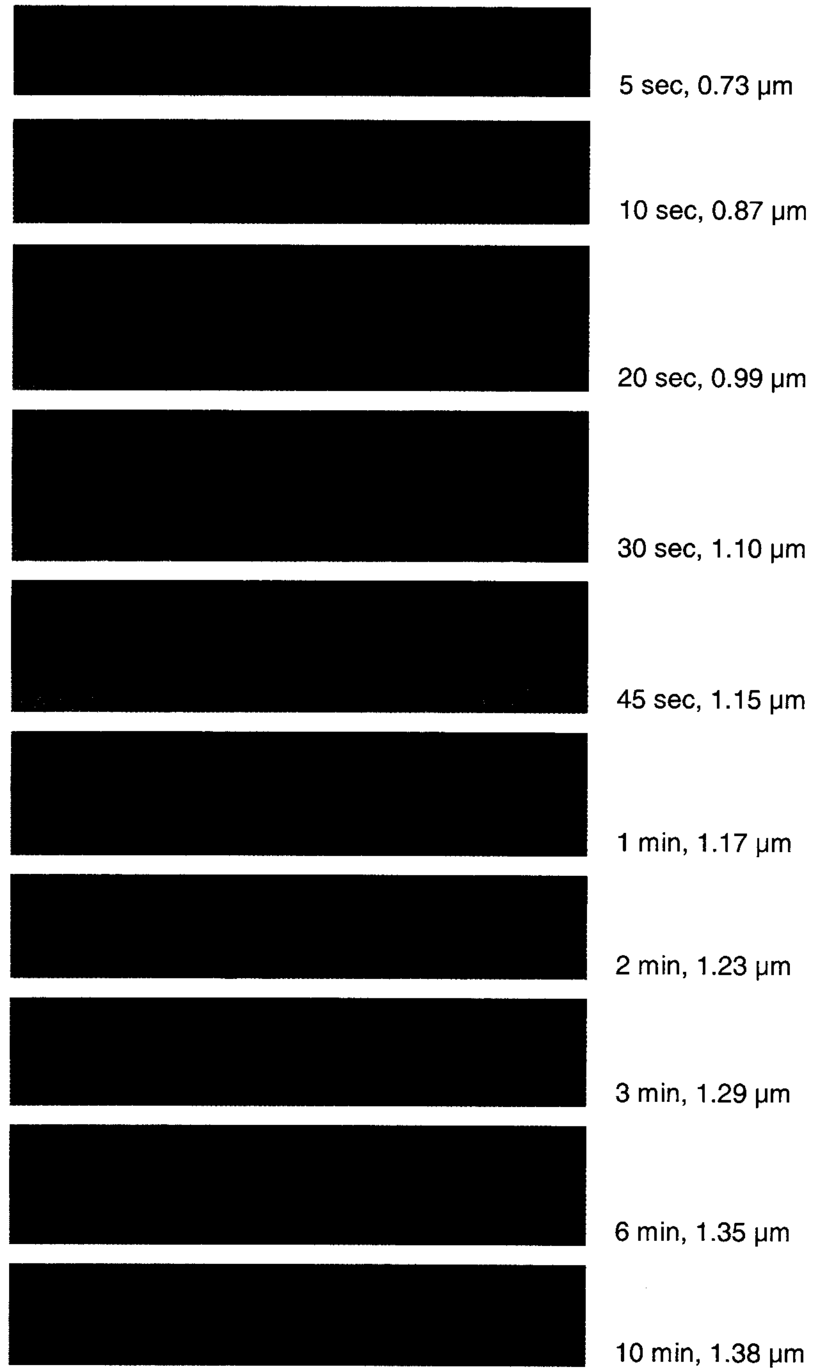

Process	Dipping
Solder:	Pure Sn
Solder Temp.:	250 °C

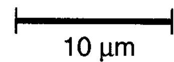

Figure 4.2 (b): Micrographs showing the IMC layer at varying dwell time. The dwell time and average IMC thickness is written by each micrograph

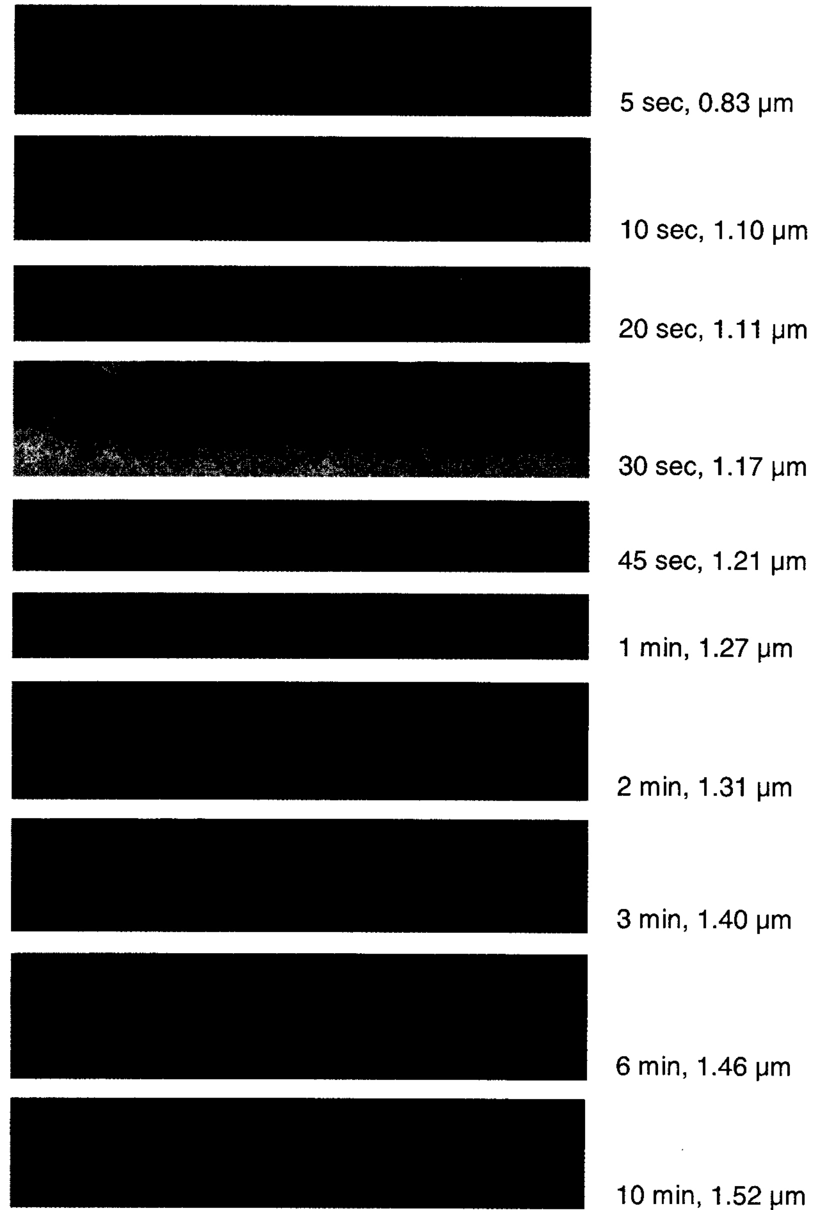

Process	Dipping
Solder:	Pure Sn
Solder Temp.:	275 °C

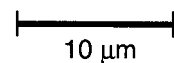

Figure 4.2 (c): Micrographs showing the IMC layer at varying dwell time. The dwell time and average IMC thickness is written by each micrograph

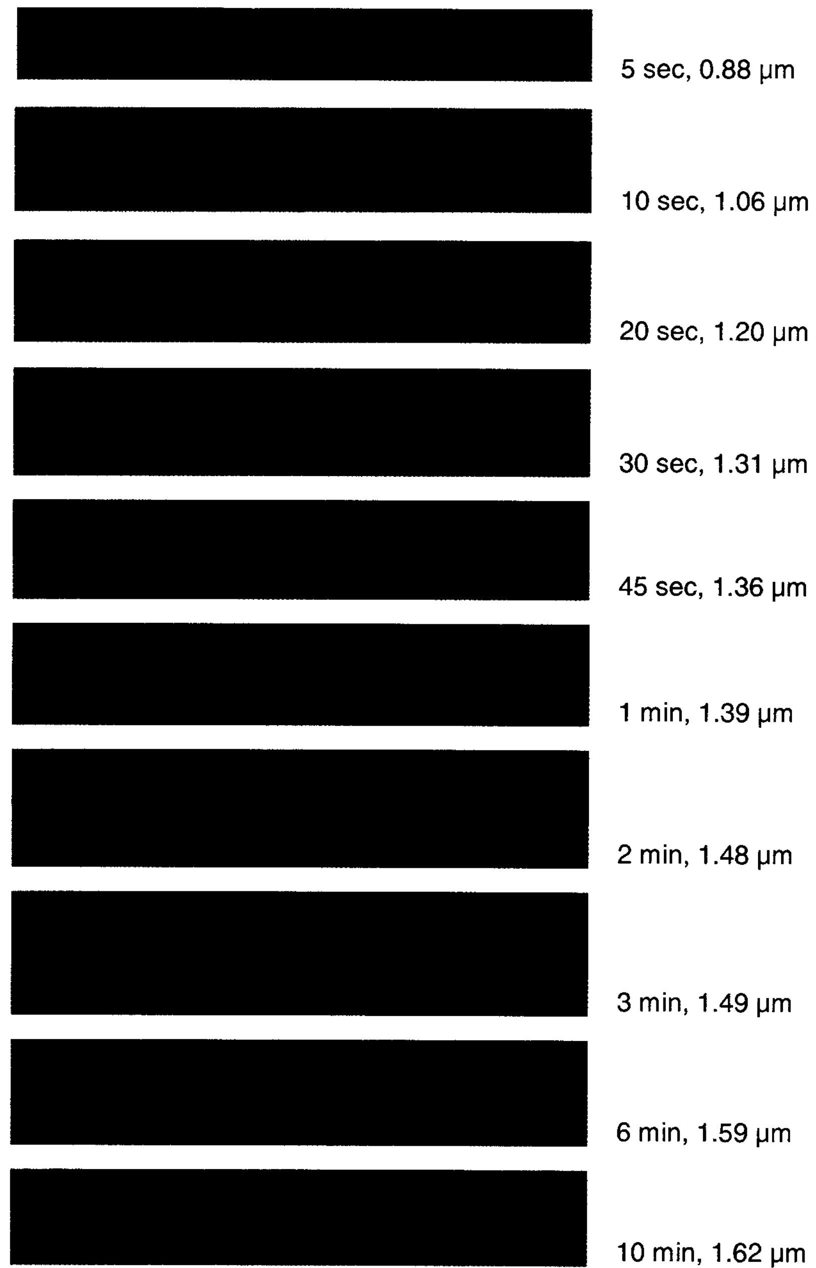

Process	Dipping
Solder:	Pure Sn
Solder Temp.:	300 °C

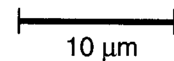

Figure 4.2 (d): Micrographs showing the IMC layer at varying dwell time. The dwell time and average IMC thickness is written by each micrograph

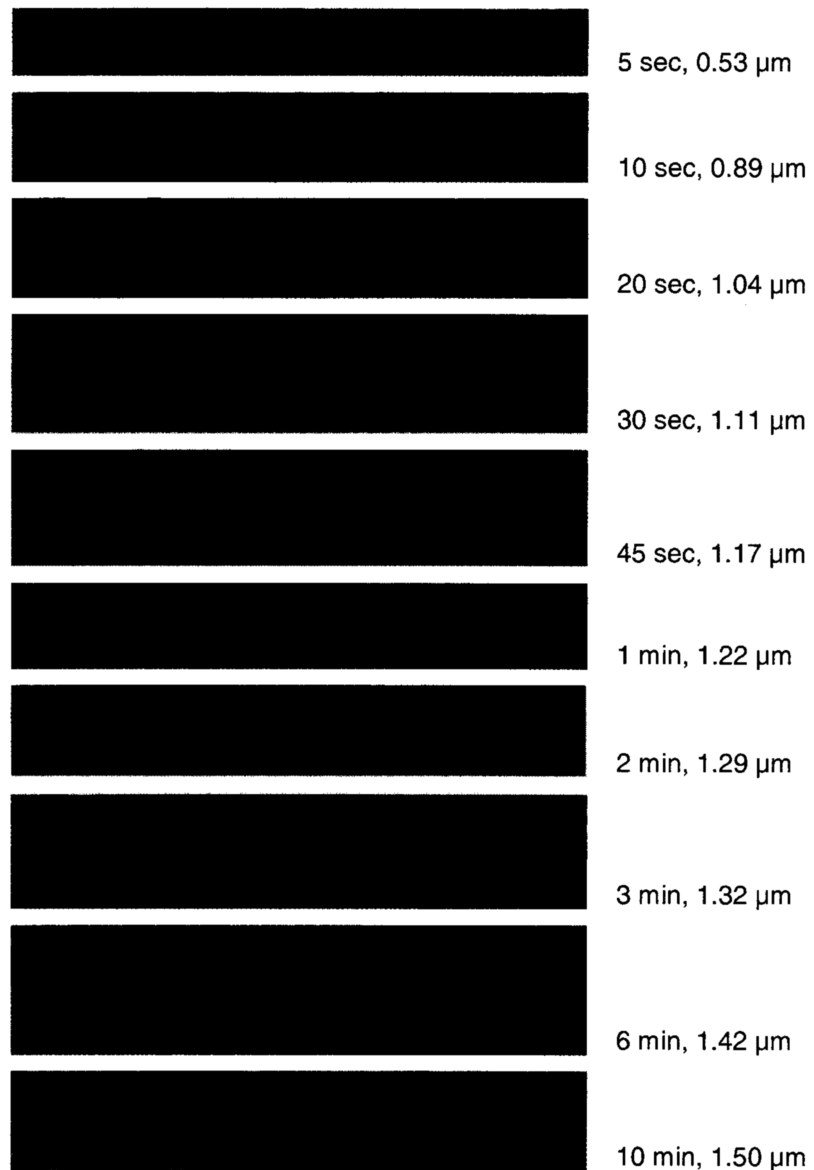

Process	Dipping
Solder:	Sn-3.5% Ag
Solder Temp.:	221 °C

Figure 4.3 (a): Micrographs showing the IMC layer at varying dwell time. The dwell time and average IMC thickness is written by each micrograph

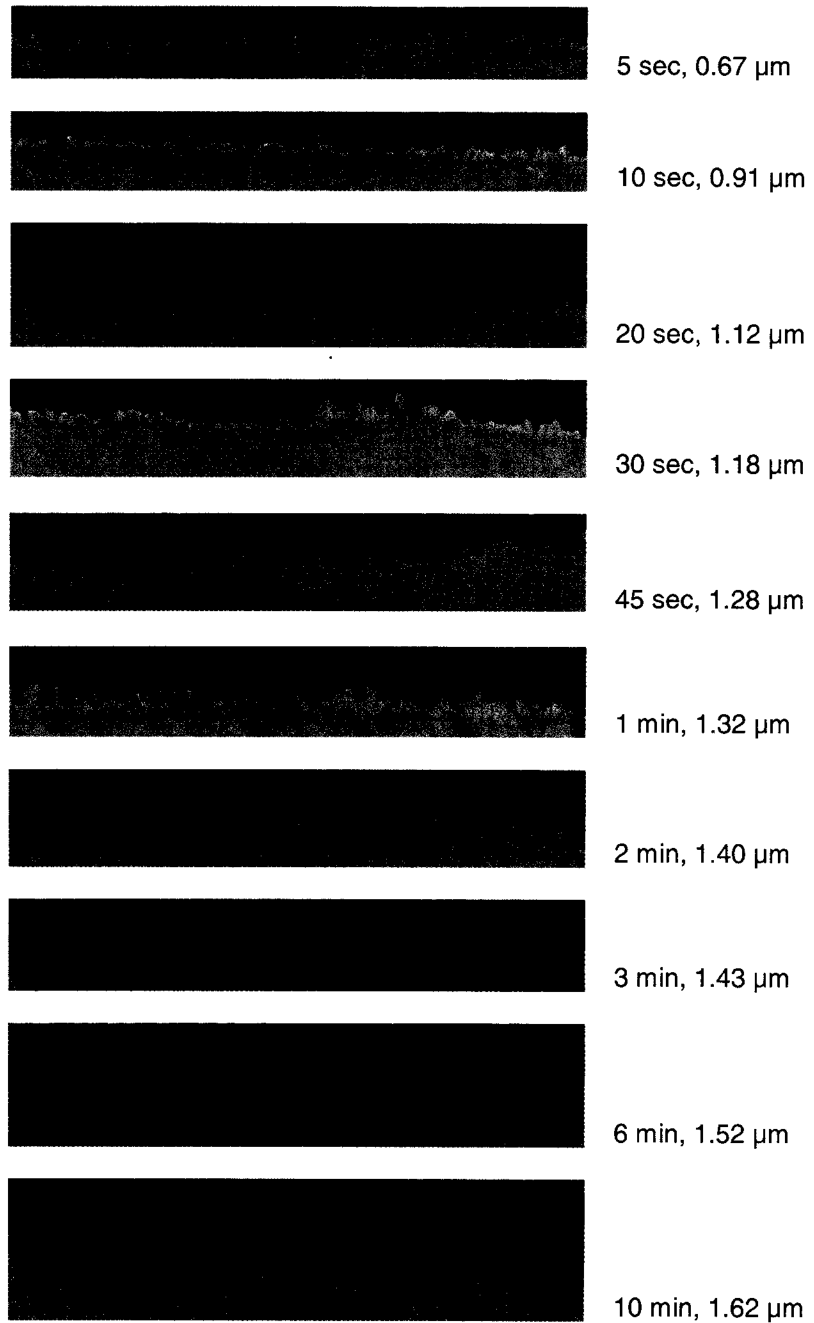

Process	Dipping
Solder:	Sn-3.5% Ag
Solder Temp.:	250 °C

10 µm

Figure 4.3 (b): Micrographs showing the IMC layer at varying dwell time. The dwell time and average IMC thickness is written by each micrograph

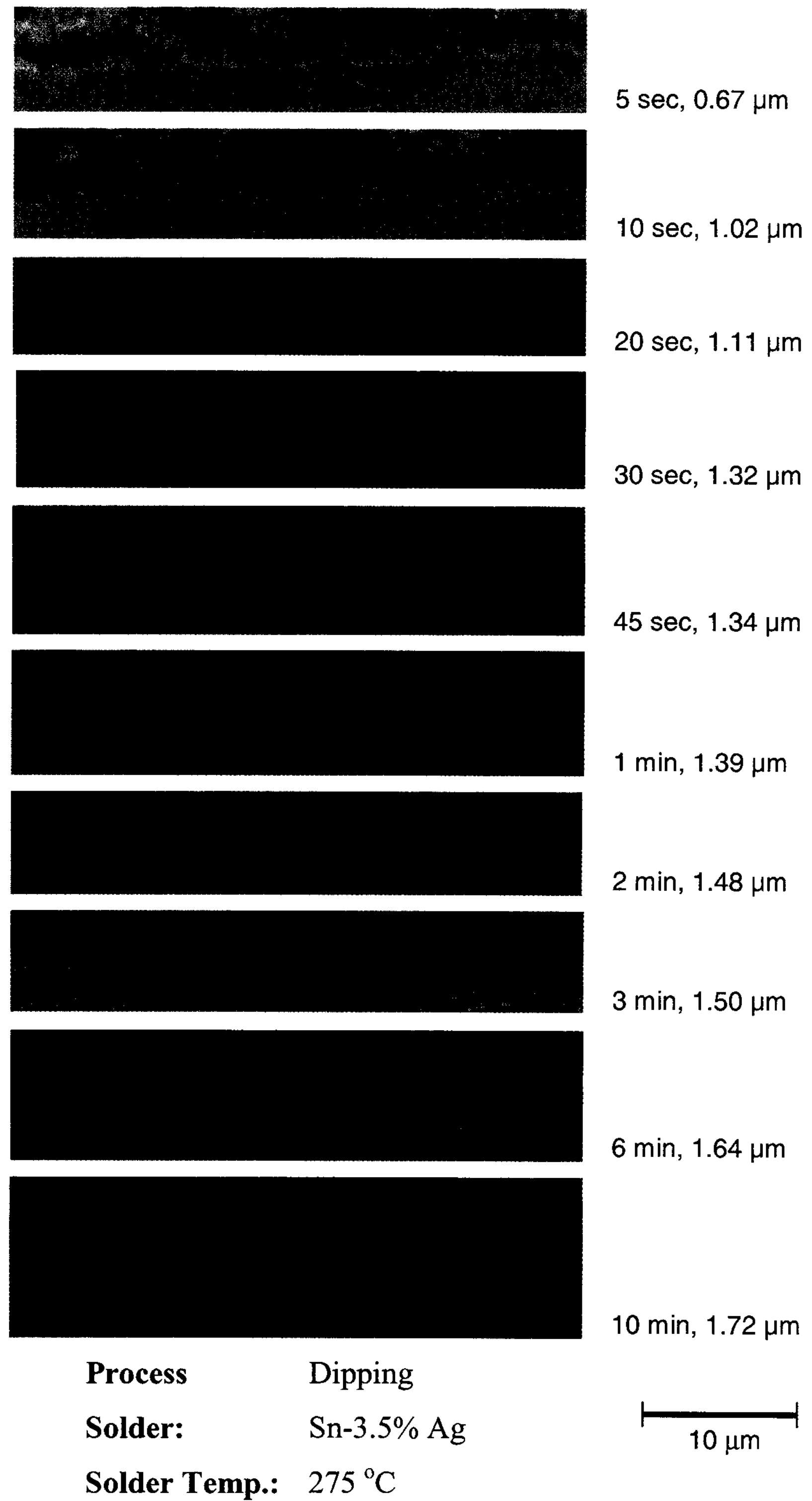

Figure 4.3 (c): Micrographs showing the IMC layer at varying dwell time. The dwell time and average IMC thickness is written by each micrograph

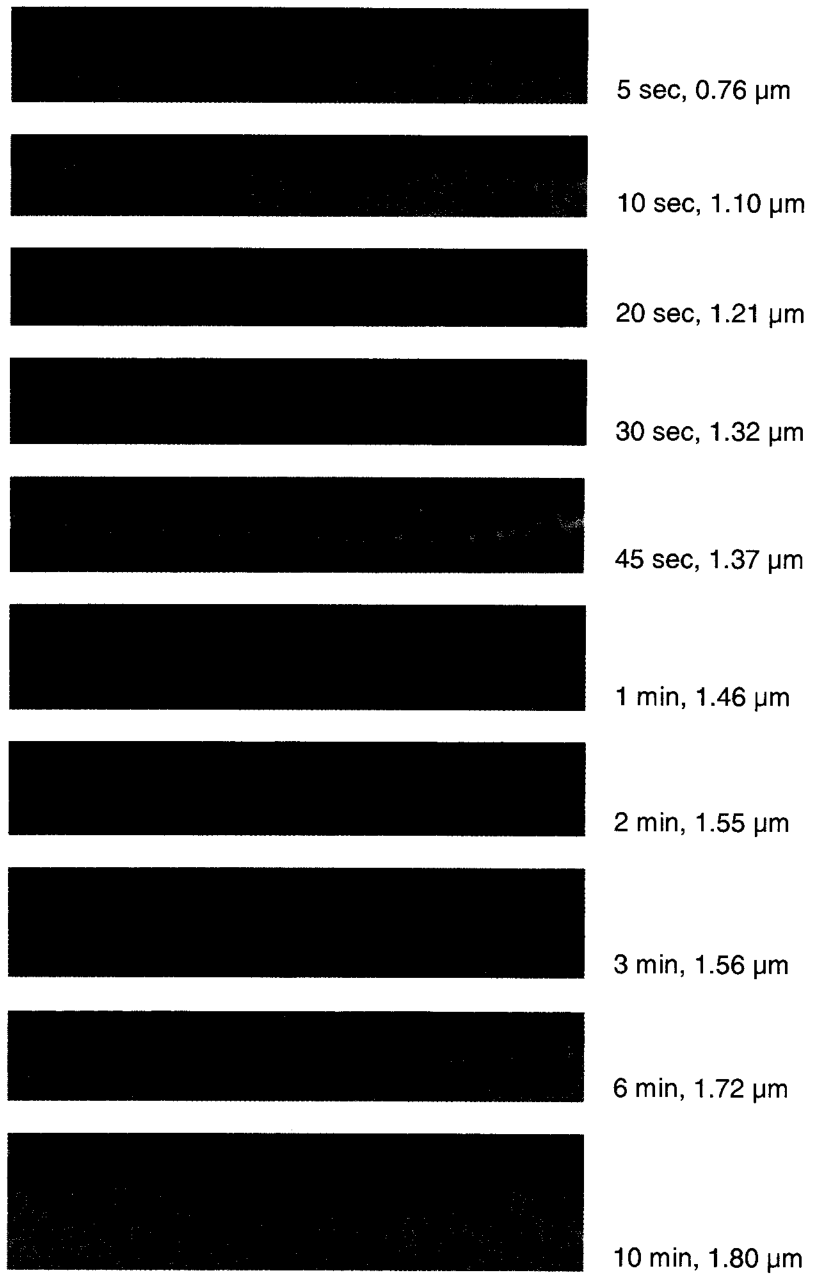

Process Dipping
Solder: Sn-3.5% Ag
Solder Temp.: 300 °C

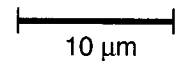

Figure 4.3 (d): Micrographs showing the IMC layer at varying dwell time. The dwell time and average IMC thickness is written by each micrograph

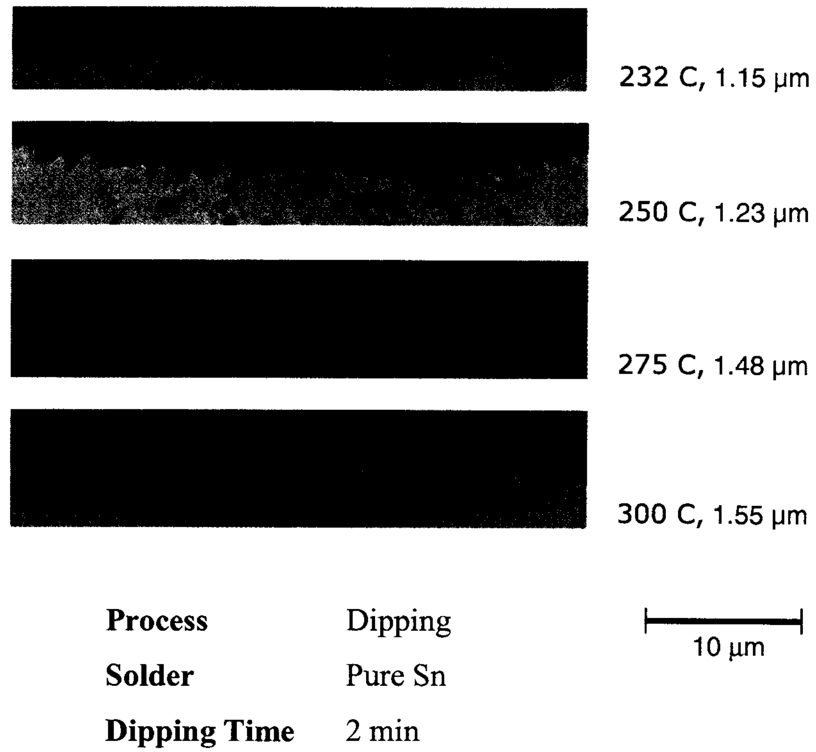

Figure 4.4 (a): Micrographs showing the effect of temperature on IMC thickness for the same dwell time. The corresponding average IMC thickness is given by each micrograph

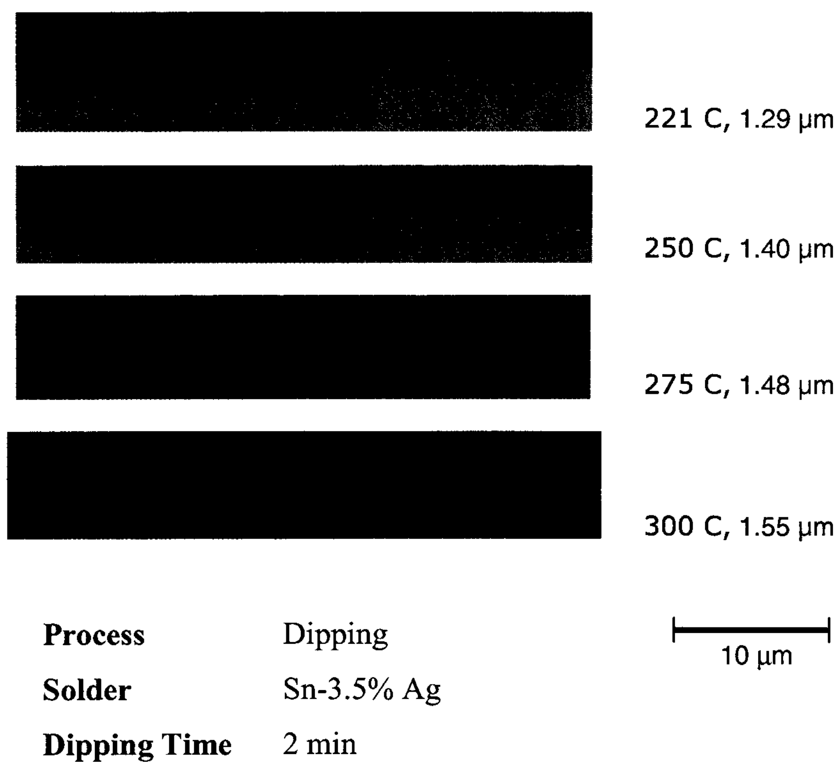

Figure 4.4 (b): Micrographs showing the effect of temperature on IMC thickness for the same dwell time. The corresponding average IMC thickness is given by each micrograph

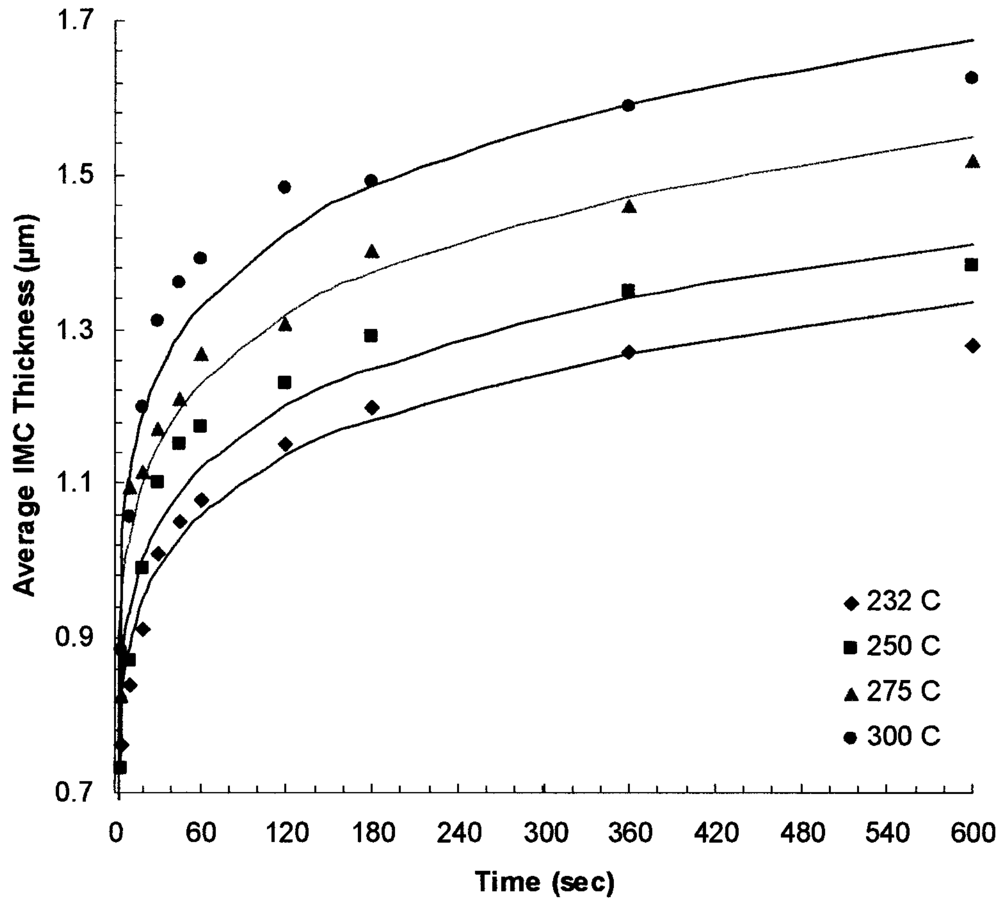

Process	Dipping
Solder Composition	Pure Sn

Figure 4.5 (a): Average intermetallic layer thickness, x as a function of dwell time, t at different solder temperatures. Curves represent fits of the data with the equation $x = Dt^{0.1}$ with rms value of 0.98 for each curve.

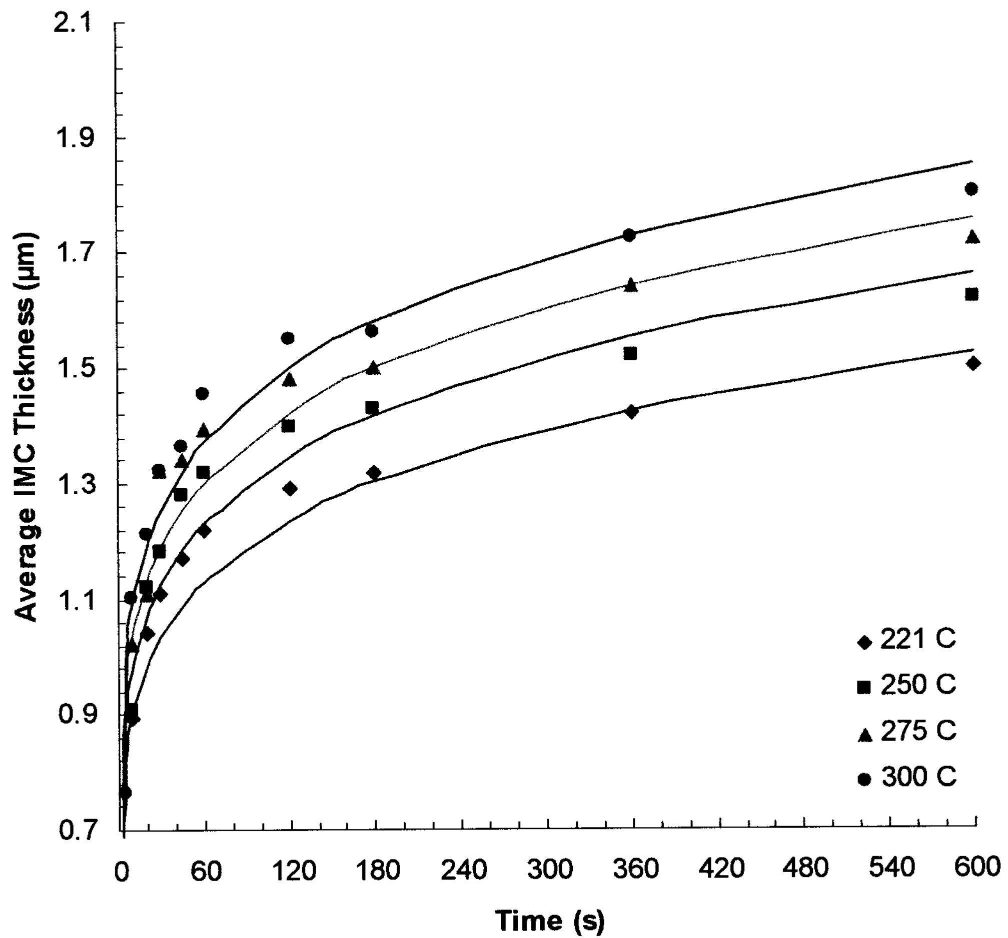

Process	Dipping
Solder Composition	Sn-3.5%wt Ag

Figure 4.5 (b): Average intermetallic layer thickness, x as a function of dwell time, t at different solder temperatures. Curves represent fits of the data with the equation $x=Dt^{0.13}$ with rms values of 0.94, 0.96, 0.95 and 0.97 for the curves at temperatures 221 °C, 250 °C, 275 °C and 300 °C respectively.

4.2 Reflow Process

The growth of IMC for pure Sn and Sn-3.5%Ag during reflow process can be visualized in Figures 4.6 and Figures 4.7 respectively. These micrographs show the increasing thickness of IMC at various solder temperatures. The corresponding dwell time and the resultant average IMC layer thickness are also given for each photograph. It was observed that, at a given process temperature, the thickness of the IMC layer was a strong function of dwell time for both solders. The average IMC layer thickness increased with increasing dwell time.

The solder material showed an important influence on both thickness of the IMC layer and the interface morphology. It can clearly be seen in the micrographs (Figure 4.6 and 4.7) that a thicker intermetallic compound layer was obtained when Sn-Ag alloy was reflowed over copper. This observation clearly indicates that the addition of silver actually favors growth of intermetallic compound.

Temperature of the molten solder is another important parameter which controls the growth of the intermetallic compound layer Figure 4.8 (a) and (b) show the end IMC layer thickness for both solders during reflow process at different temperatures but for the same dwell time. It was observed that a higher solder temperature yield greater IMC thickness.

Figures 4.9 (a) and (b) show the evolution of thickness of the intermetallic compound layer for reflow process, as function of the dwell time at different temperature. The IMC growth curves demonstrate a strong function of dwell time and temperature of the solder.

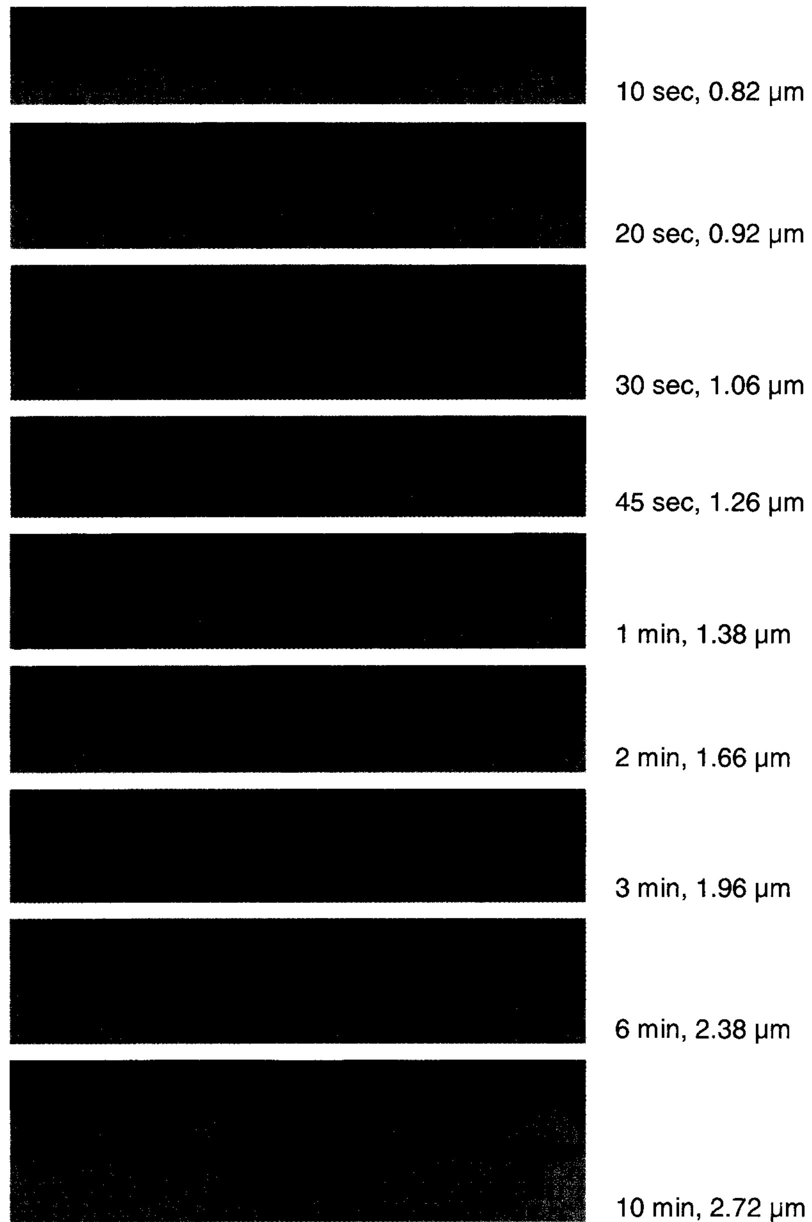

Process	Reflow
Solder:	Pure Sn
Solder Temp.:	232 °C

10 µm

Figure 4.6 (a): Micrographs showing the IMC layer at varying dwell time. The dwell time and average IMC thickness is written by each micrograph

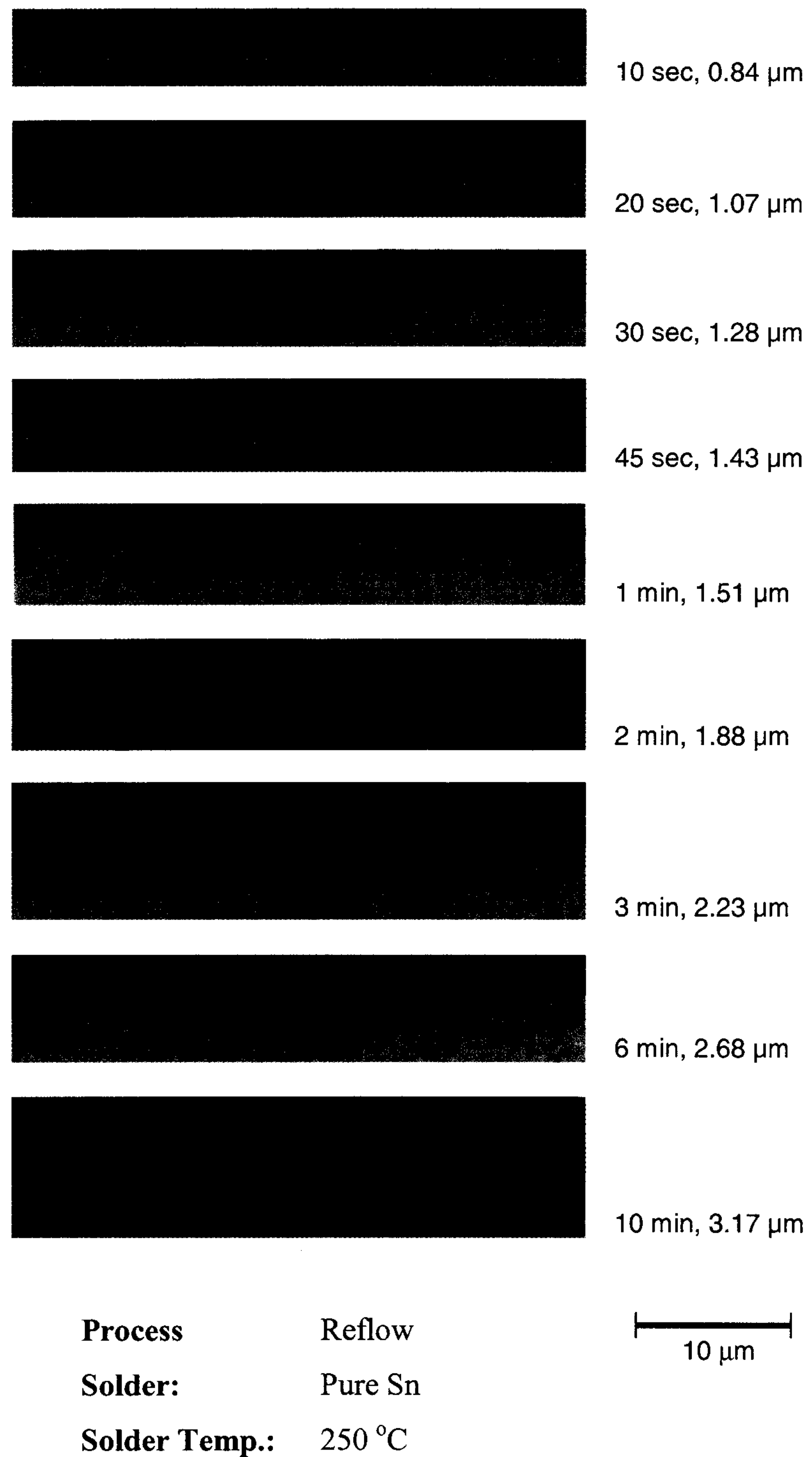

Figure 4.6 (b): Micrographs showing the IMC layer at varying dwell time. The dwell time and average IMC thickness is written by each micrograph

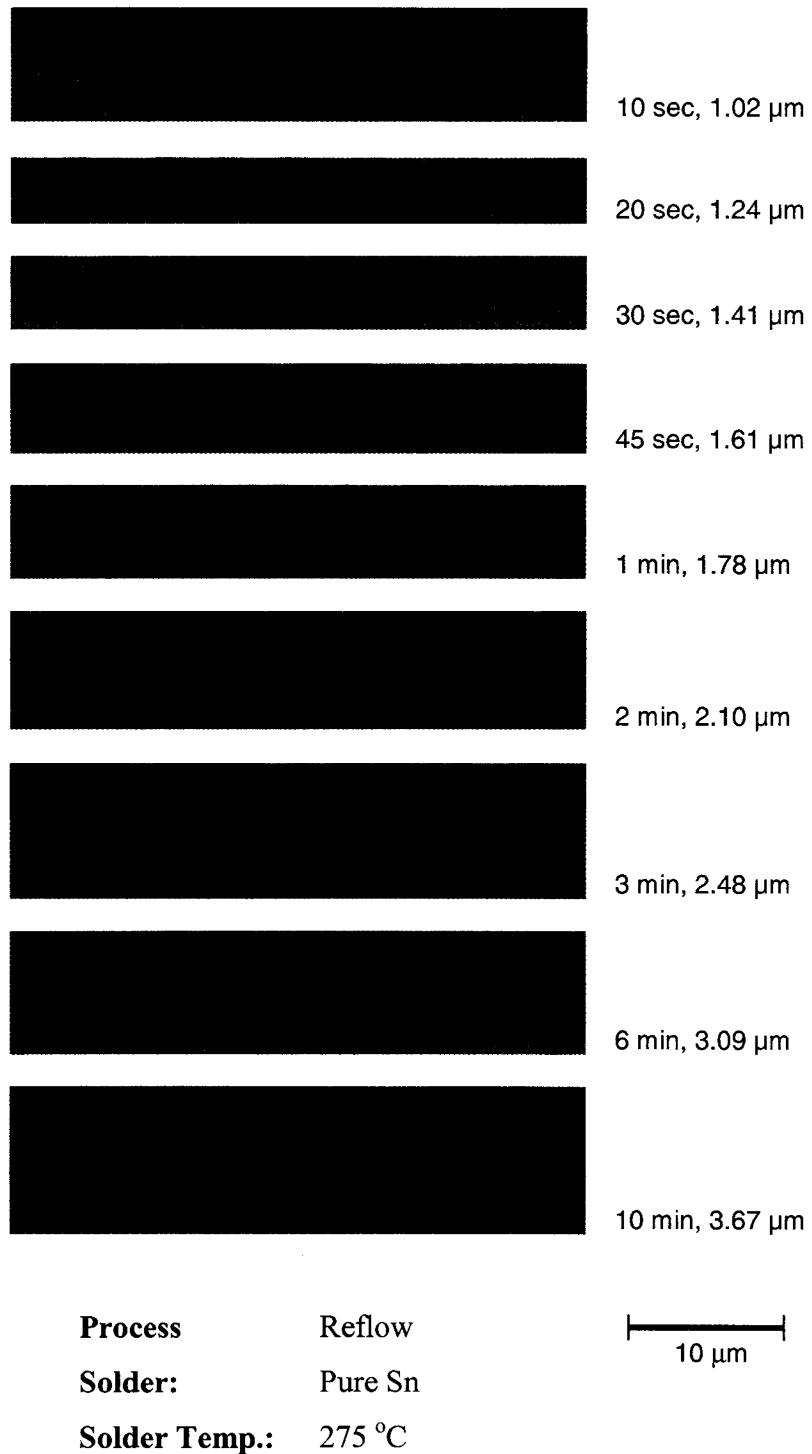

Process	Reflow
Solder:	Pure Sn
Solder Temp.:	275 °C

Figure 4.6 (c): Micrographs showing the IMC layer at varying dwell time. The dwell time and average IMC thickness is written by each micrograph

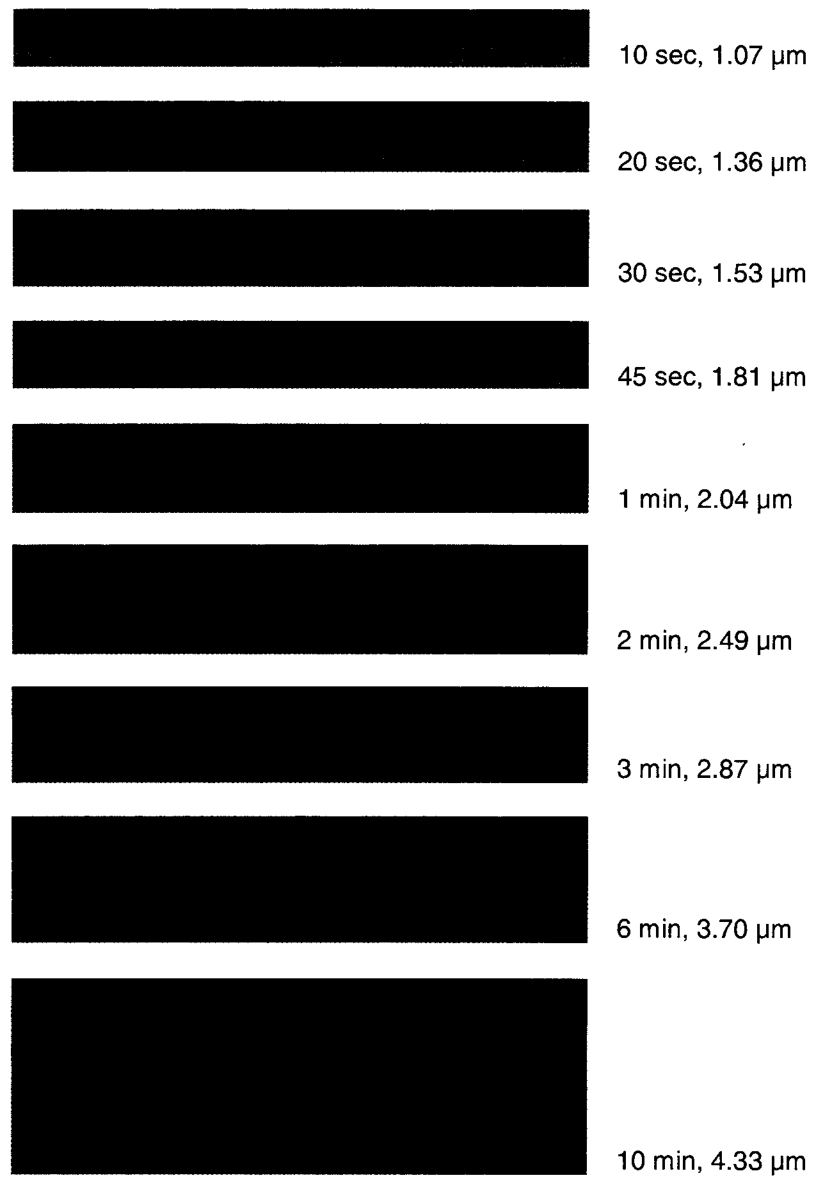

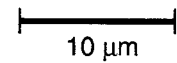

Process	Reflow
Solder:	Pure Sn
Solder Temp.:	300 °C

Figure 4.6 (d): Micrographs showing the IMC layer at varying dwell time. The dwell time and average IMC thickness is written by each micrograph

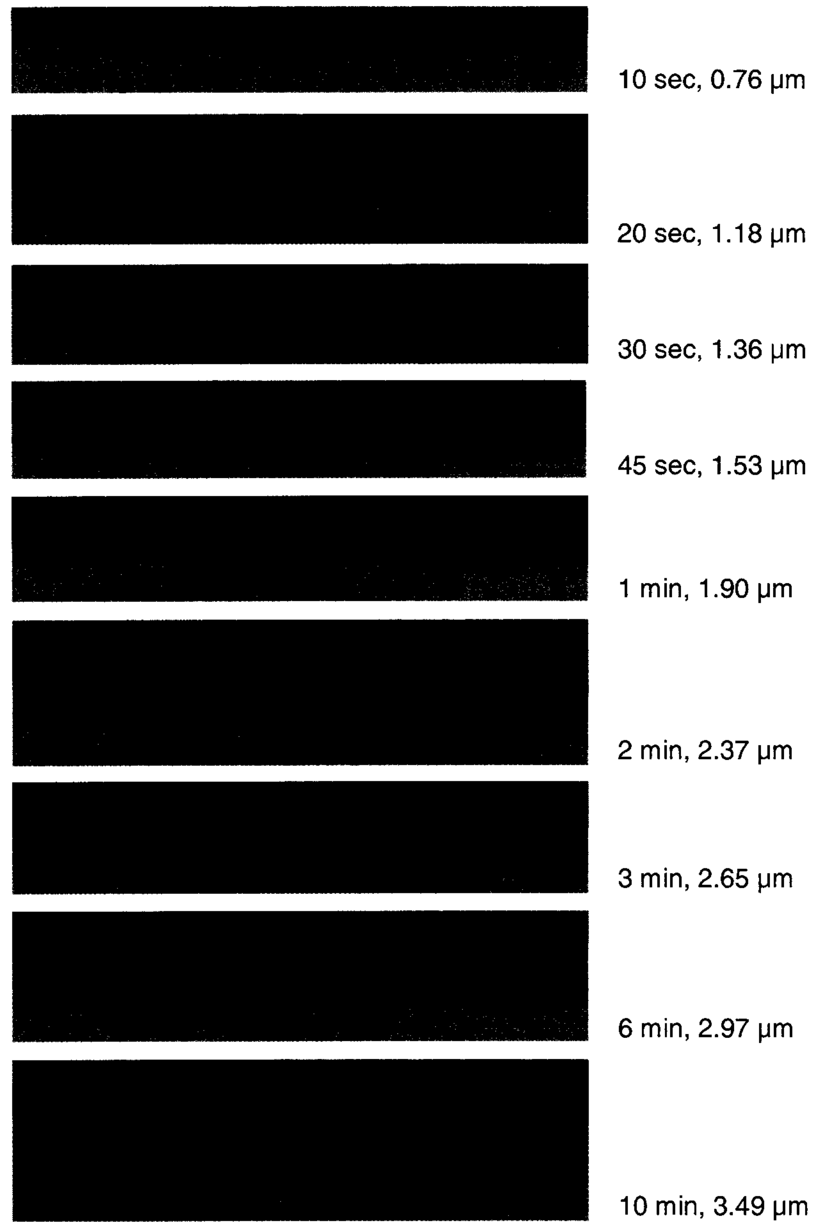

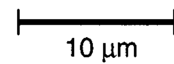

Process	Reflow
Solder:	Sn-3.5% Ag
Solder Temp.:	221 °C

Figure 4.7 (a): Micrographs showing the IMC layer at varying dwell time. The dwell time and average IMC thickness is written by each micrograph

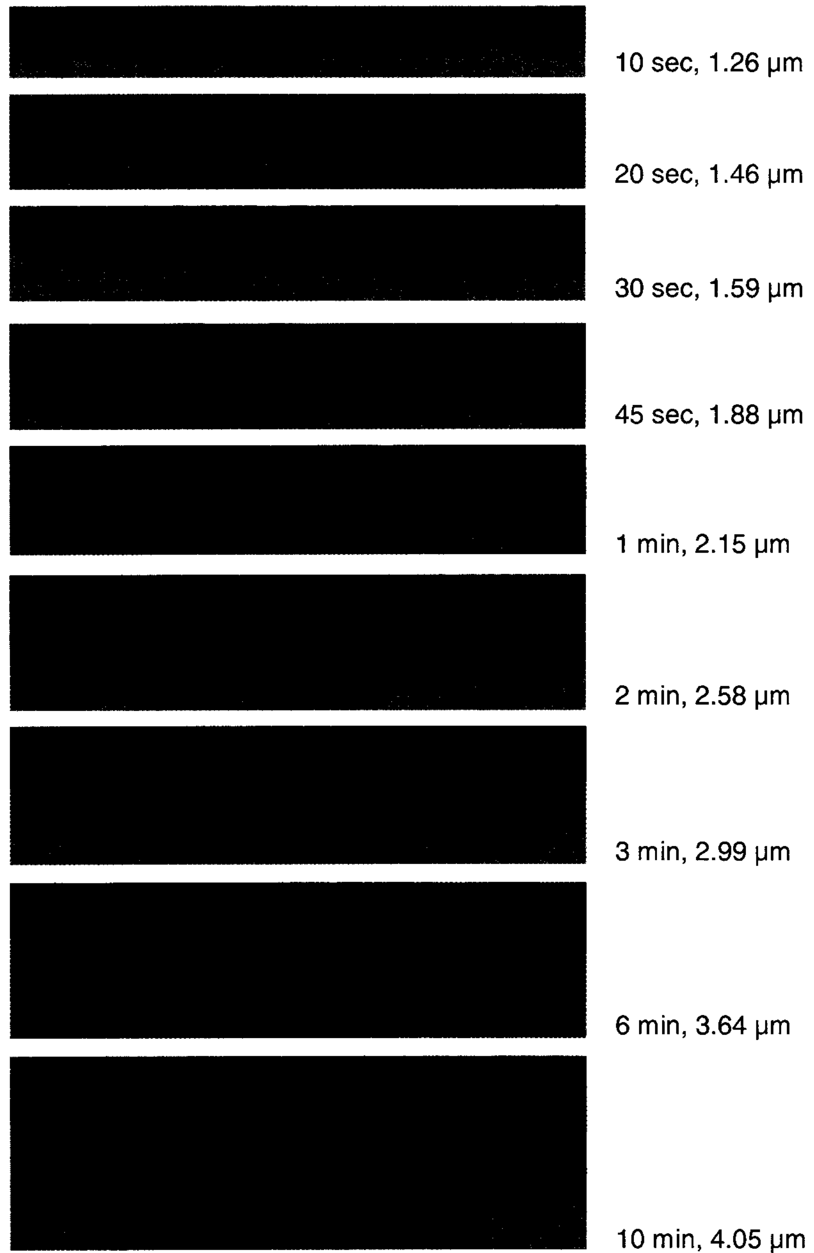

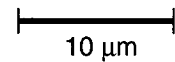

Process	Reflow
Solder:	Sn-3.5% Ag
Solder Temp.:	250 °C

Figure 4.7 (b): Micrographs showing the IMC layer at varying dwell time. The dwell time and average IMC thickness is written by each micrograph

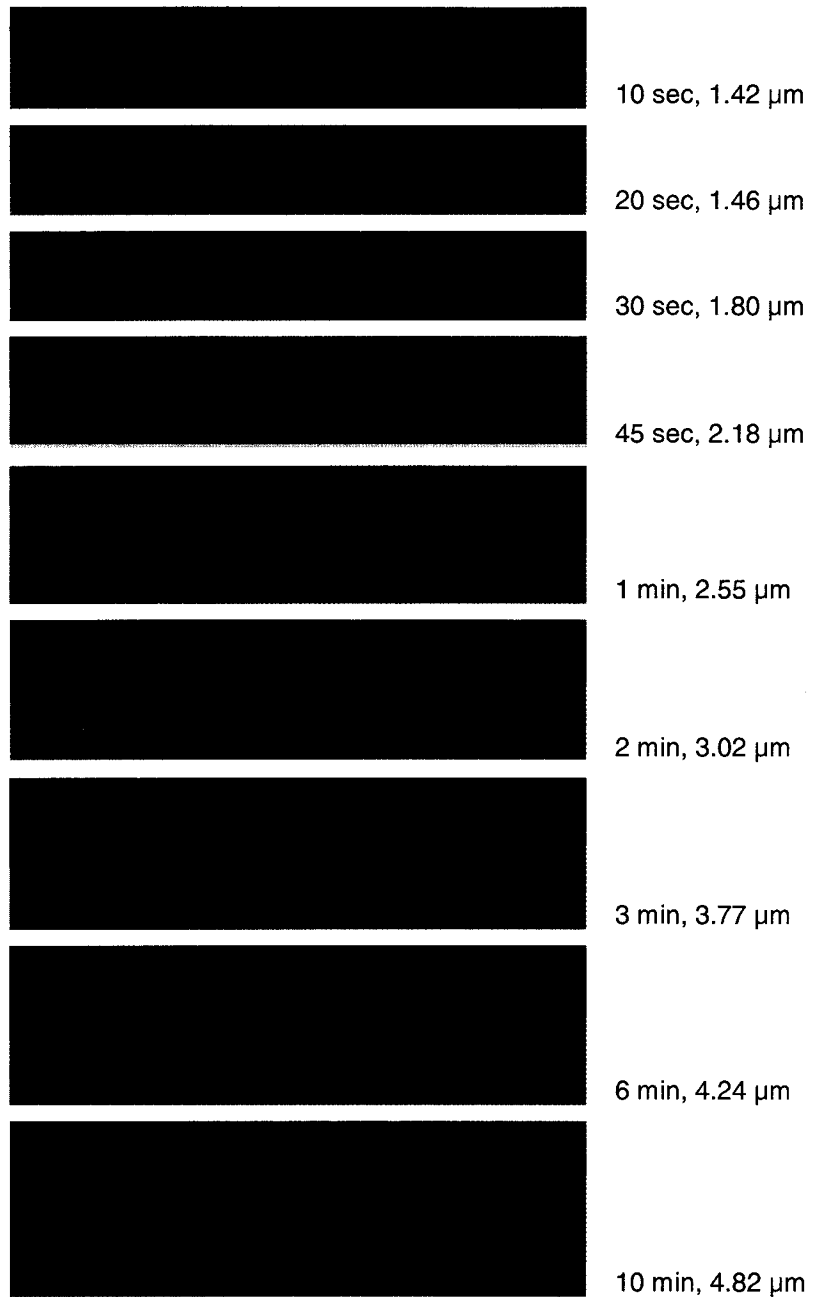

Process Reflow

Solder: Sn-3.5% Ag

Solder Temp.: 275 °C

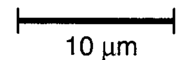

Figure 4.7 (c): Micrographs showing the IMC layer at varying dwell time. The dwell time and average IMC thickness is written by each micrograph

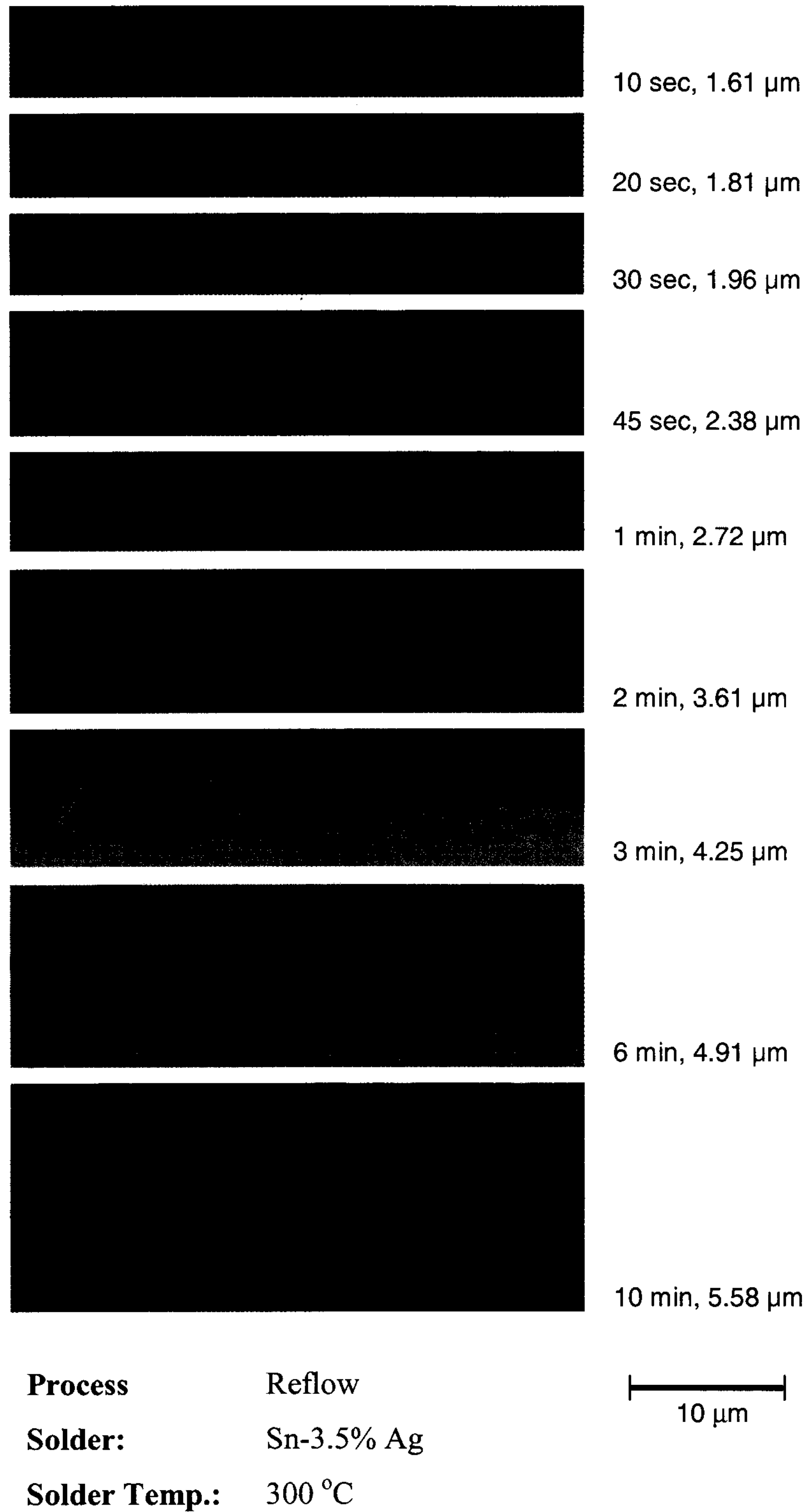

Figure 4.7 (d): Micrographs showing the IMC layer at varying dwell time. The dwell time and average IMC thickness is written by each micrograph

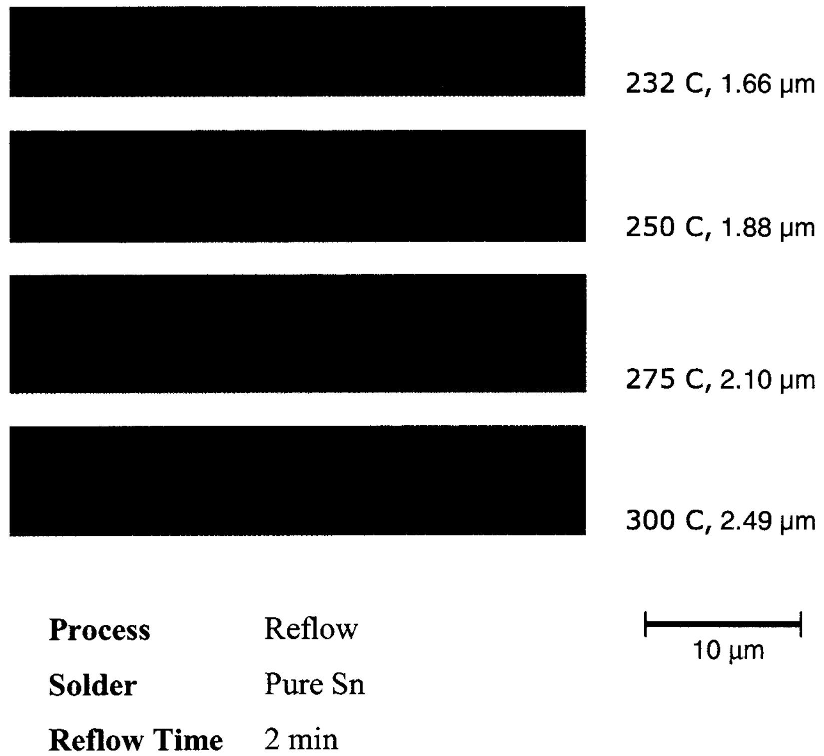

Figure 4.8 (a): Micrographs showing the effect of temperature on IMC thickness for the same dwell time. The corresponding average IMC thickness is given by each micrograph

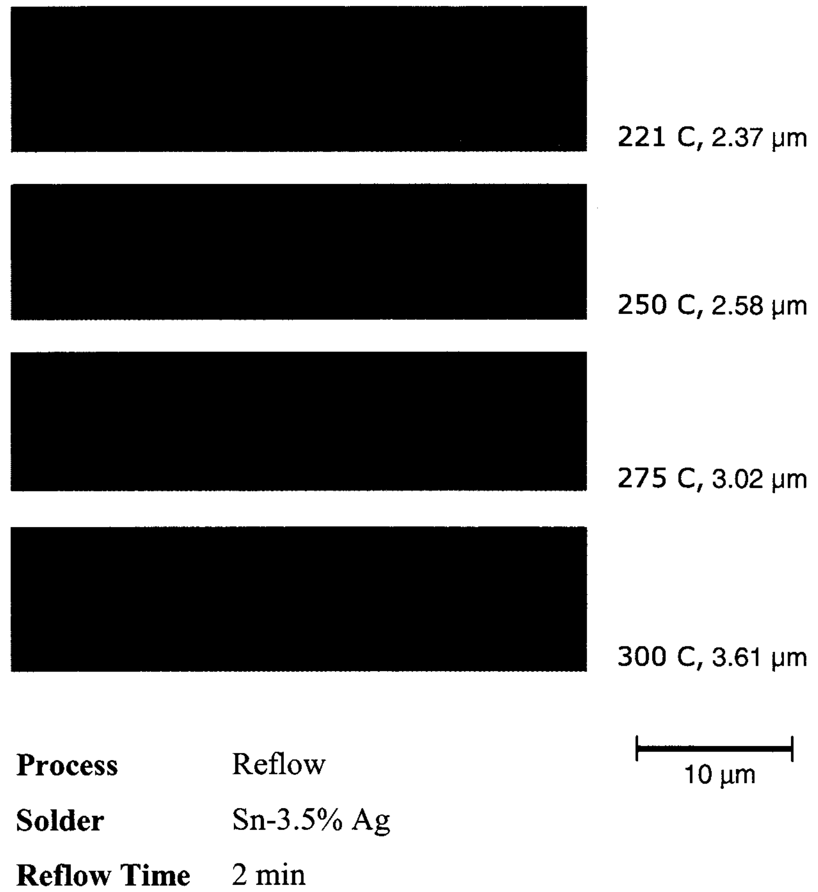

Figure 4.8 (b): Micrographs showing the effect of temperature on IMC thickness for the same dwell time. The corresponding average IMC thickness is given by each micrograph

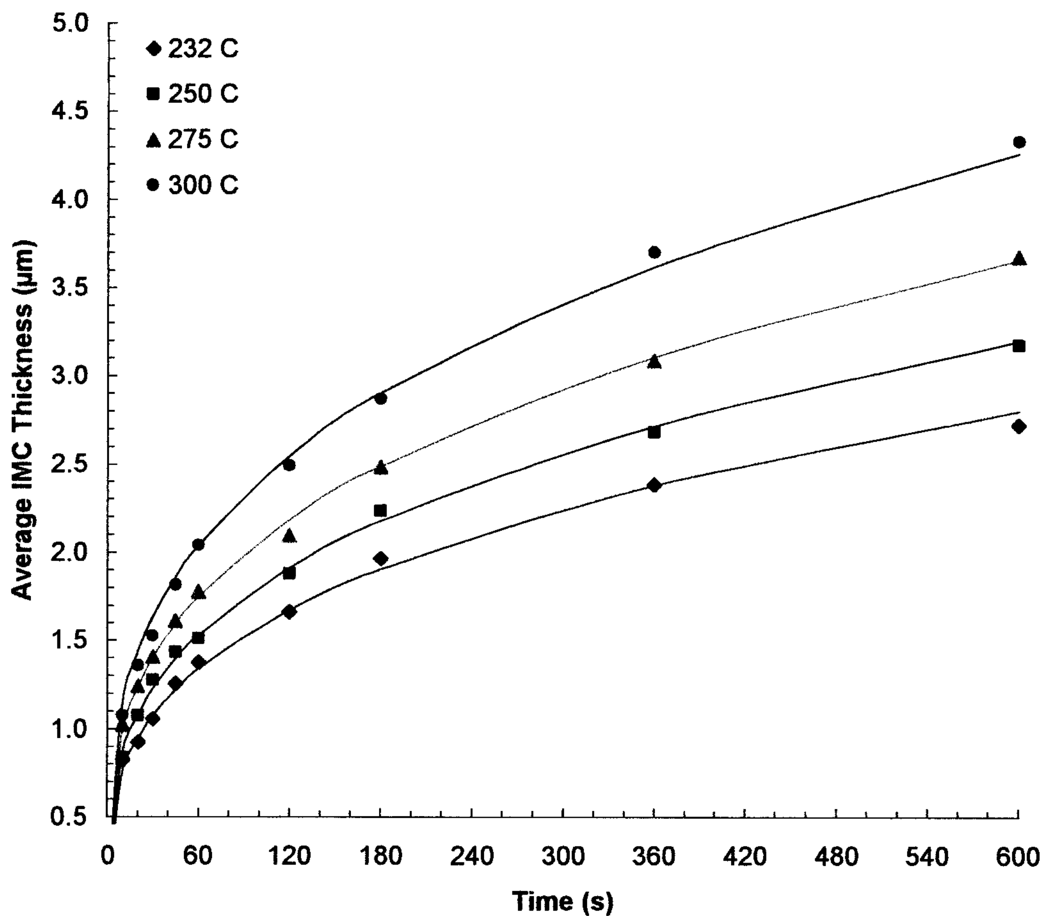

Process	Reflow
Solder Composition	Pure Sn

Figure 4.9 (a): Average intermetallic layer thickness, x as a function of dwell time, t at different solder temperatures. Curves represent fits of the data with the equation $x=Dt^{0.32}$ with rms value of 0.99 for each curve.

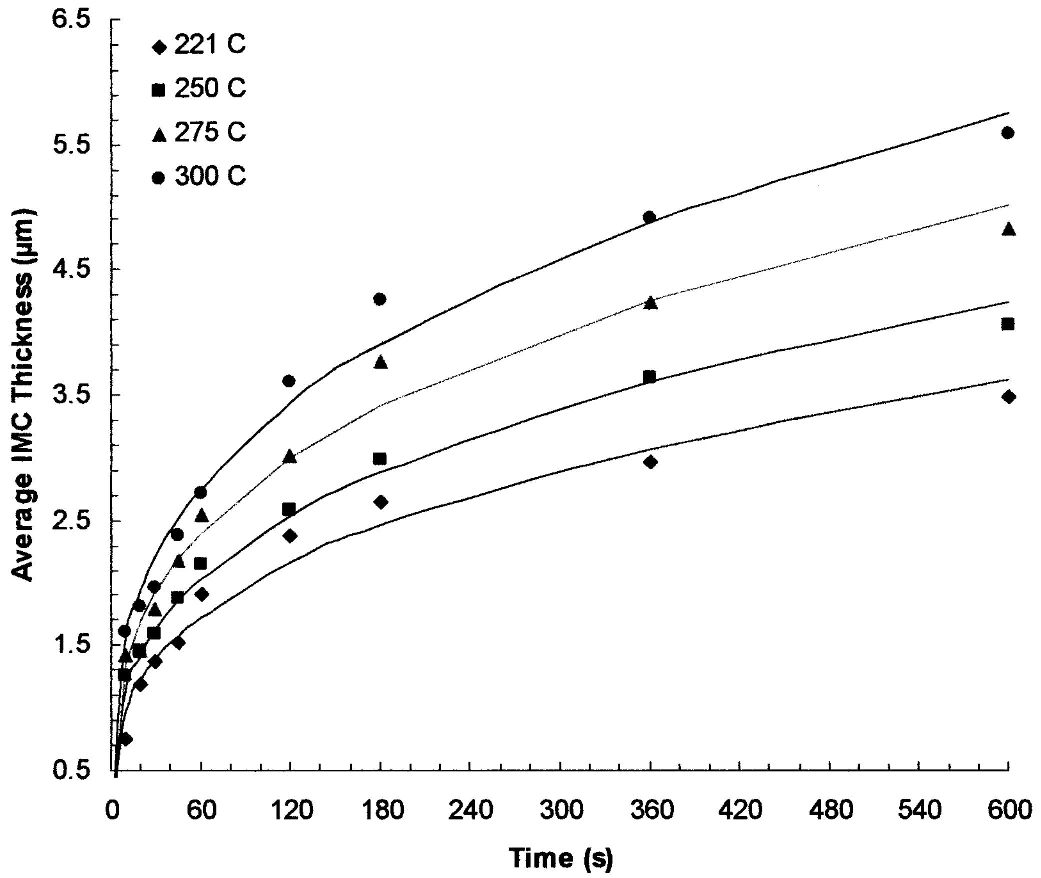

Process	Reflow
Solder Composition	Sn-3.5%wt Ag.

Figure 4.9 (b): Average intermetallic layer thickness, x as a function of dwell time, t at different solder temperatures. Curves represent fits of the data with the equation $x=Dt^{0.32}$ with rms value of 0.98 for each curve.

The average intermetallic compound layer thickness increased with dwell time and solder temperature. The IMC growth curves show a rising trend during the initial stage and then gradually flatten during the terminal stages. The recorded initial high growth rate of the intermetallic compound layer is ascribed to the diffusion of tin along grain boundaries of the fine IMC grains formed at the beginning of IMC layer growth. As the IMC grains became thicker and coarser, diffusion of tin to the copper substrate became difficult, resulting in overall decrease in IMC growth rate.

4.3 Morphology of Intermetallic Compound

The intermetallic compound layer did not grow as a regular layered structure. Rather, the Cu_6Sn_5 phase grew as scallop like grains within the molten solder. Overall, the intermetallic compound interface morphology was observed to be fairly smooth with round scallops for pure tin. However, for the Sn-3.5%Ag solder, the interface became significantly irregular and rough needle like scallops, particularly for the cases involving a lengthy dwell time. Both ε-phase (Cu_3Sn) and η-phase (Cu_6Sn_5) were observed in the intermetallic layer in pure Sn and Sn-Ag solder, during reflow process.

Figure 4.10: Micrograph showing the presence of ε and η-phases in IMC

The thin, uniform and continuous ε-phase was more visible at high solder temperature and longer dwell time. This is due to the reason that for thermodynamic considerations, the driving force for η-phase formation is higher than that for ε-phase formation [23]. As the temperature increases, the difference between the two driving forces decreases, making it thermodynamically favorable to form ε-phase [12]. Also the nucleation of the ε-phase at the interface is difficult at lower temperatures [23]. Another reason for the formation of the ε-phase at higher temperature and/or longer dwell time could be its high Cu:Sn ratio of 3:1. Due to high Cu:Sn ratio, one can expect the ε-phase formation when the Sn atoms are in short supply. This condition is met when the η-phase grows thicker at high temperature and/or longer dwell time. Thus the overall kinetics of ε-phase formation may be too slow at the lower temperatures and/or short dwell time. However, formation of η-phase was observed in all conditions [24].

4.4 Effect of Type of Process on IMC Growth

The average intermetallic thickness recorded in the present dipping experiments is lower than that for the reflow process. The difference in the estimated values of the average IMC thickness could be attributed to the fact that, in a reflow process, the amount of solder is limited; and it takes a finite time period for the solder to melt and attain a desired temperature making effect on IMC growth. In addition, in the present set of dipping experiments, the copper substrates were held in the solder bath, placed in an enclosed furnace. The temperature of the solder varied within a range of $\pm 2^{o}C$, consequently, low current convection can exist in the solder bath. These convection currents could be responsible for transporting away the intermetallic compound from near the copper substrate, thus reducing the overall growth of the IMC.

It is noted that the parameter, *n,* is important in determining the initial rate of IMC growth. A low value of *n* for the dipping experiments determined in the present study explains the growth rate of IMC to be very high during the initial stages at all temperatures.

CHAPTER - 5

COPPER DISSOLUTION DURING THE PROCESS

5.1 Dipping Process

In the present study, reduction in thickness of copper substrate during dipping process was considered a measure of the total copper dissolution into molten solder. Charts in Figures 5.1 (a) and 5.1 (b) show the dissolution rate of copper during dipping process for pure Sn and Sn-3.5wt%Ag solders respectively, as function of dwell time at different solder temperatures. It was observed that for a given solder temperature, the dissolution rate of copper in molten solder showed a rising trend with an increase in dwell time. For a short period of time, at the beginning, the dissolution rate was low and thickness of the resulting intermetallic compound was thin. As the dwell time increased, the dissolution rate of copper also increased. A further increase in dwell time essentially slowed down the dissolution rate at all temperatures. However, the existence of a non-linear variation in actual measured dissolution rate in dipping experiments, with respect to dwell time, suggests the intricate physics governing the dissolution of copper at different stages of the process.

At the beginning when copper is in contact with the molten solder, the copper starts dissolving into molten solder with the concurrent formation of a layer of Sn-Cu intermetallic compound on the copper surface. The latter suppresses further direct contact of the copper substrate with the molten solder. When the solder around copper is saturated with copper, further dissolution of copper is prevented. The dissolution of copper is profoundly affected by the growth of intermetallic compound.

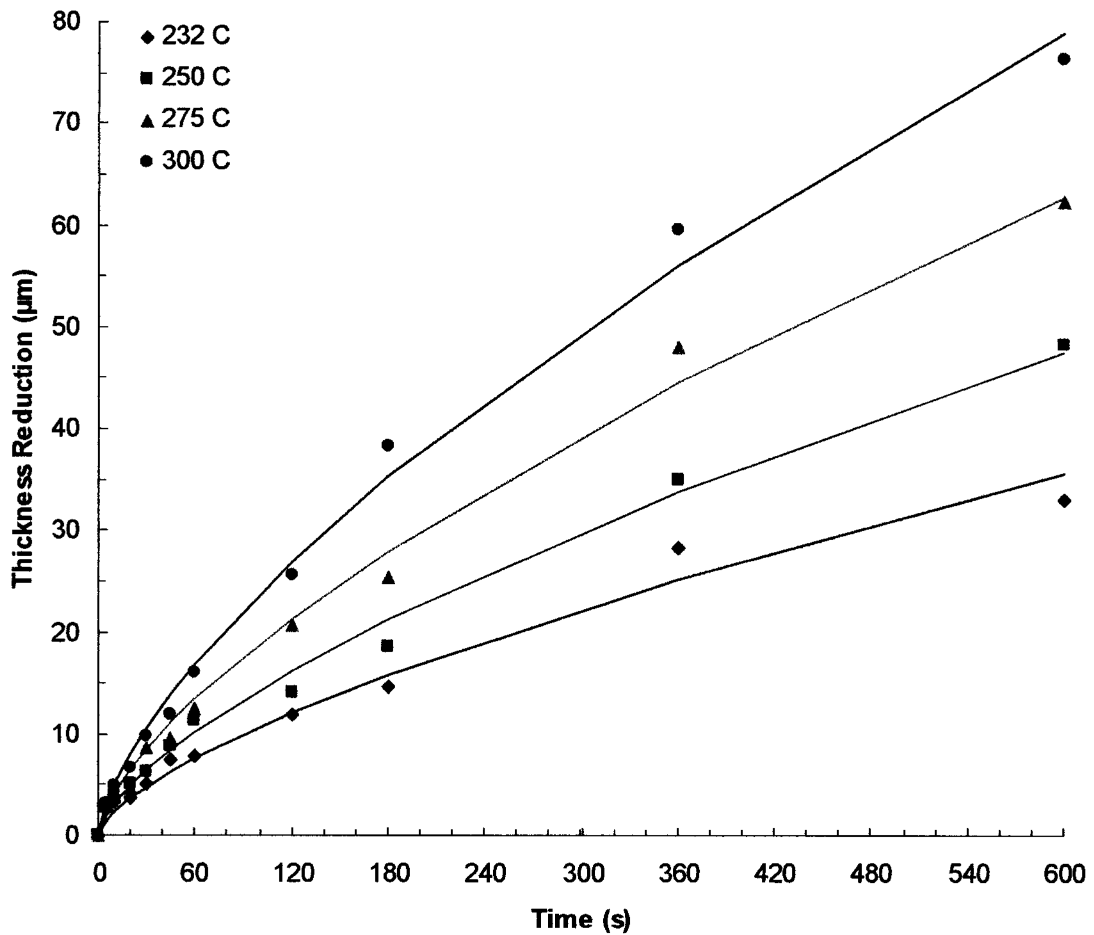

Process	Dipping
Solder Composition	Pure Sn

Figure 5.1 (a): Average reduction in copper thickness, x as a function of dwell time, t at different solder temperatures. Curves represent fits of the data with the equation $x=Dt^{0.67}$ with rms value of 0.98 for each curve.

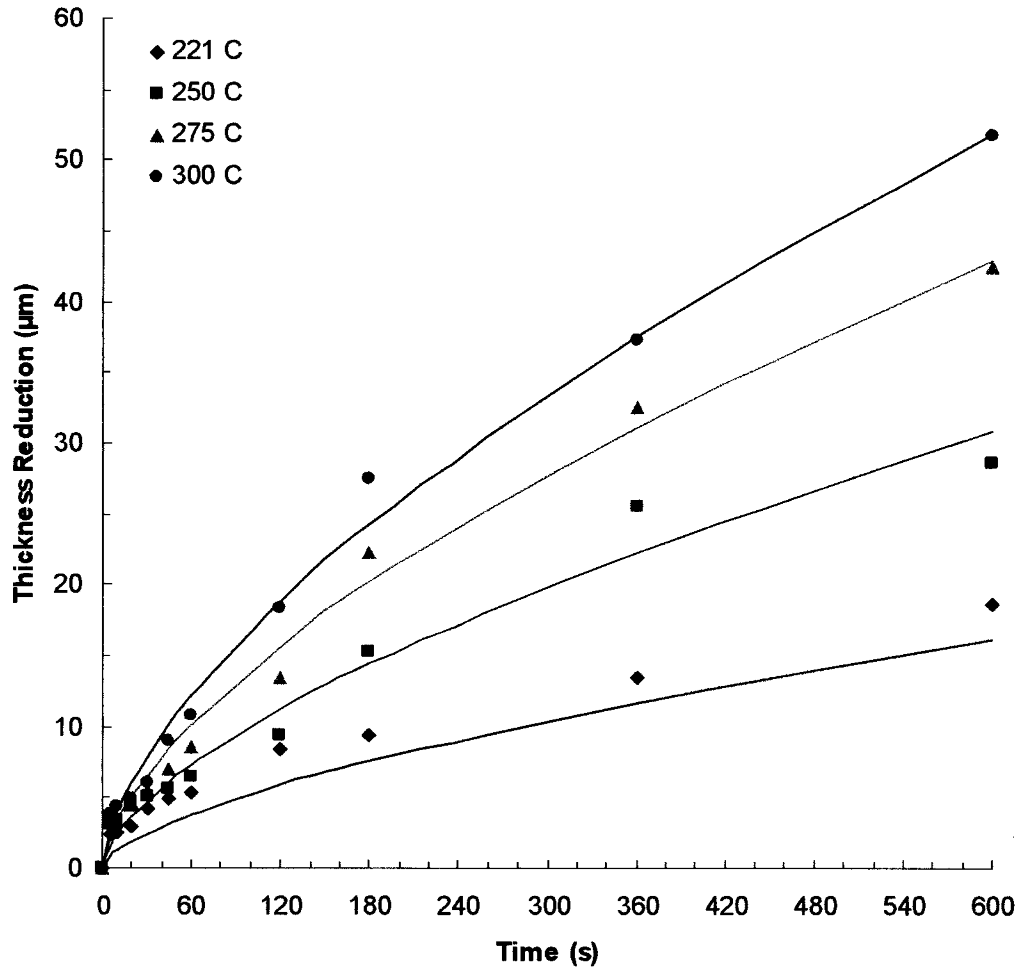

Process	Dipping
Solder Composition	Sn-3.5%wt Ag

Figure 5.1 (b): Average reduction in copper thickness, x as a function of dwell time, t at different solder temperatures. Curves represent fits of the data with the equation $x=Dt^{0.63}$ with rms value of 0.8 for curve at 221 ^{0}C and 0.98 for curves at 250 ^{0}C, 275 ^{0}C and 300 ^{0}C.

It was also observed, during dipping process, that the solder around the reinforcing copper was saturated easily at the lower temperatures. This difference in saturation rates is due to the reason that, at high temperatures, due to higher temperature difference within the solder bath, convection currents may exist. These currents may transport away the saturated Sn around the copper substrate, and replace it with fresh Sn, thereby, decreasing the saturation rate of the solder around the copper.

5.2 Reflow Process

Thickness reduction of copper substrate during reflow process was considered a measure of the total copper dissolution into the solder. Charts in Figure 5.2 (a) and Figure 5.2 (b) show the dissolution rate of copper during reflow process for pure Sn and Sn-3.5wt%Ag solder respectively, as function of dwell time at different process temperatures. It was observed that for a given process temperature, the dissolution rate of copper in molten solder showed a positive trend with an increase in dwell time in the early stages of reflow and became flat at higher dwell times.

At the beginning when copper is in contact with the molten solder, the copper starts dissolving into molten solder. A layer of Sn-Cu intermetallic compound on the copper surface also starts forming simultaneously. The latter acts as a barrier and prohibits further direct contact of the copper substrate with the molten solder. When the solder around copper becomes saturated with copper, further dissolution of copper is barred. The dissolution of copper is profoundly affected by the growth of intermetallic compound.

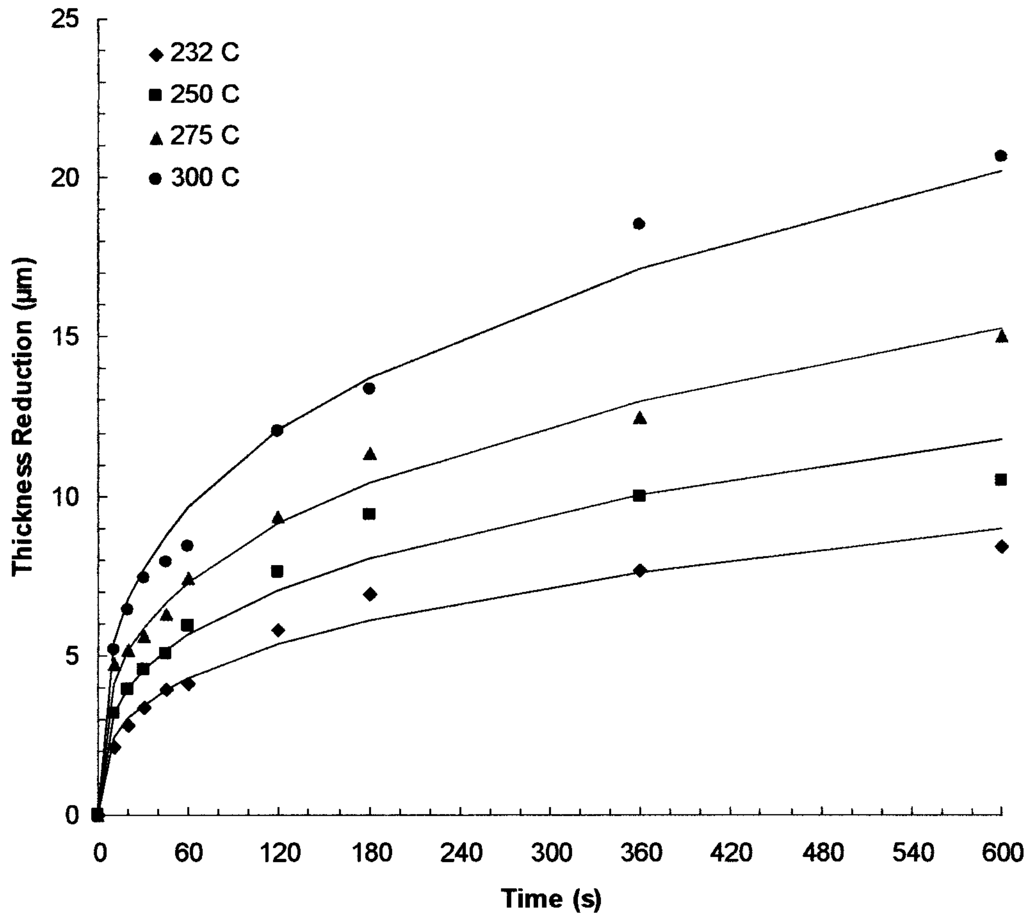

Process	Reflow
Solder Composition	Pure Sn

Figure 5.2 (a): Average reduction in copper thickness, x as a function of dwell time, t at different solder temperatures. Curves represent fits of the data with the equation $x=Dt^{0.32}$ with rms value of 0.97 for each curve.

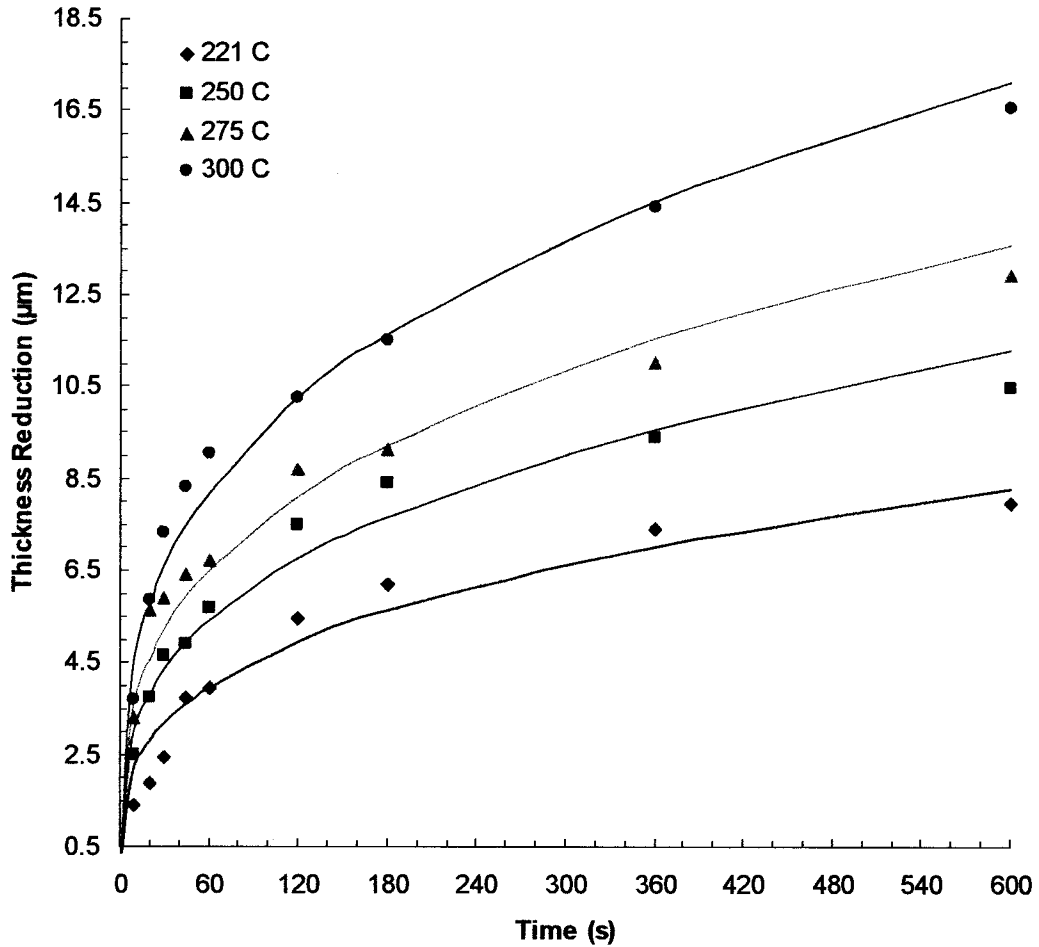

Process	Reflow
Solder Composition	Sn-3.5%wt Ag

Figure 5.2 (b): Average reduction in copper thickness, x as a function of dwell time, t at different solder temperatures. Curves represent fits of the data with the equation $x=Dt^{0.32}$ with rms value of 0.96 for each curve.

5.3 Effect of Type of Process on Copper Dissolution

It was interesting to note that the dissolution of copper in case of dipping process was much higher than during reflow process. This difference in the dissolution rate is due to the difference in the type of process involved. In the dipping process, the amount of solder around the copper is practically infinite, while for the reflow process, the amount of solder is very small and finite. Due to large amount of solder presence, the solder does not saturate for long time, and the copper continues to dissolve in the molten solder. In case of reflow process, due the small amount of solder, the solder my saturate early, thereby decreasing the rate of diffusion of copper during longer dwell times. Another reason for the observed difference in the dissolution rate of copper in the molten solder for the two processes could be the difference in the thickness of the intermetallic layer formed at the solder/copper interface. As was observed during reflow process, a thick IMC layer acts as a barrier for the diffusion of copper into solder, thus, reducing the dissolution rate of copper.

5.4 Effect of Solder Composition on Copper Dissolution

Experimental results also revealed that the dissolution rate of copper is more in pure Sn than in Sn–Ag at all temperatures. The phenomenon was observed both in dipping (Figure 5.4) and reflow process (Figure 5.5). This difference in dissolution rate is due to the reason that pure Sn reacts with copper more readily than Sn–Ag. The increased dissolution rate of copper in pure Sn solder can also be attributed to its poor wetting of pure Sn on copper. The intermetallic layer formed at the solder/copper interface acts as a barrier for the diffusion of copper into solder. When the intermetallic layer grows, the

small scallops coalesce together to make bigger scallops, but due to poor wetting, these scallops are disconnected. Due to the discontinuity of the IMC, channels (grooves) are formed in between the scallops (Figure 5.3). The channels are deeper in case of pure Sn than Sn-Ag. Molten solder can easily travel through these channels and react with the copper. As a result, diffusion of copper into molten solder is favored and the overall dissolution of copper increased. Addition of Ag into the solder, actually improves wetting of solder on copper. The improved wetting of the solder makes a continuous layer of the IMC, thereby decreasing the depth of the open channels, and a more effective barrier for diffusion of copper. The net effect is a decrease in the dissolution of copper in the molten solder.

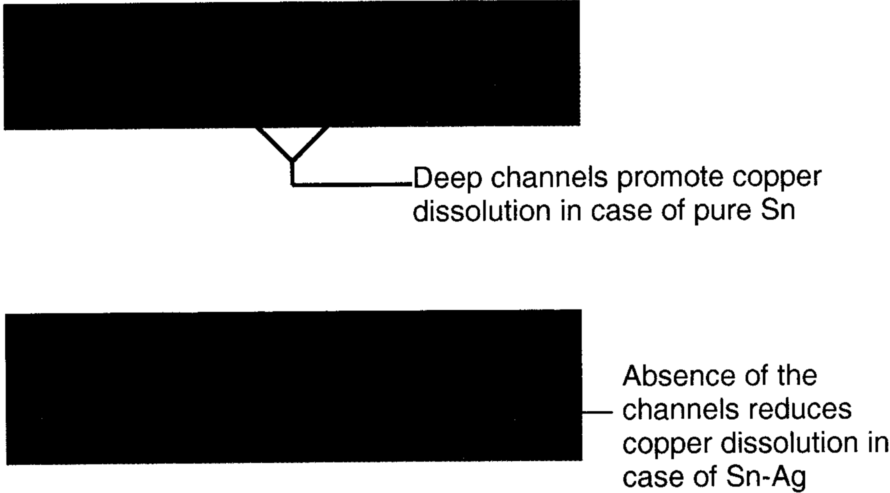

Figure 5.3: Micrographs showing the presence of open channels in IMC in pure Sn

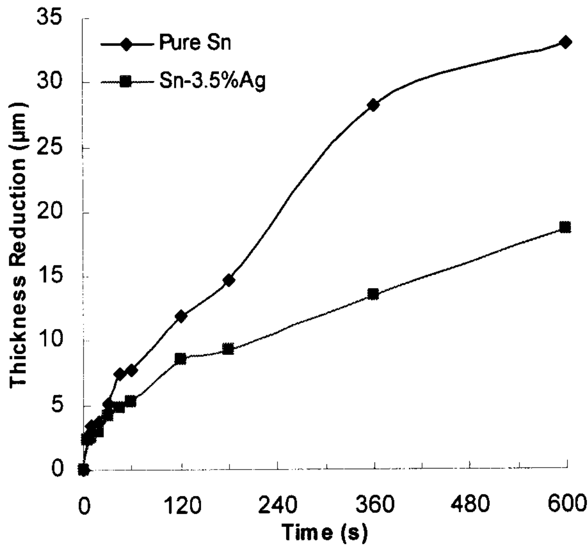

(a) At the melting point of two solders

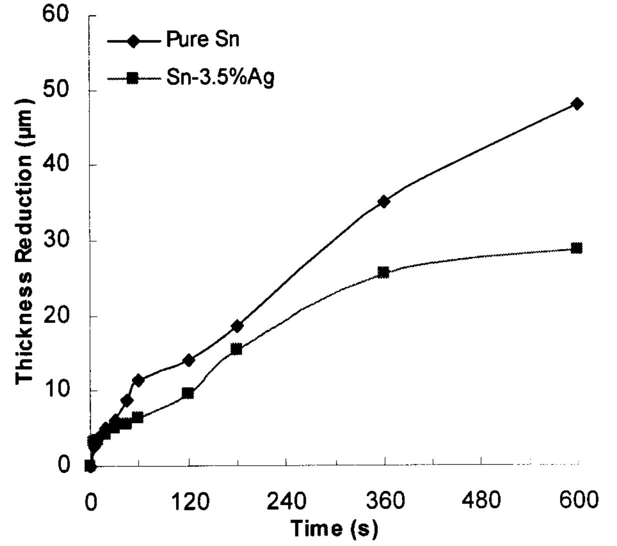

(b) 250 °C

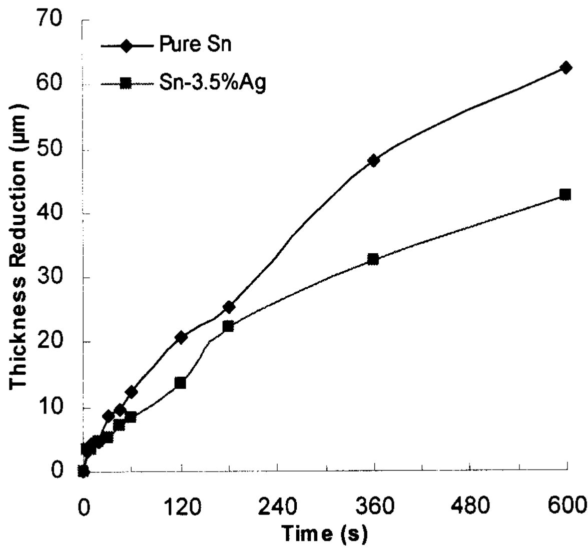

(c) 275 °C

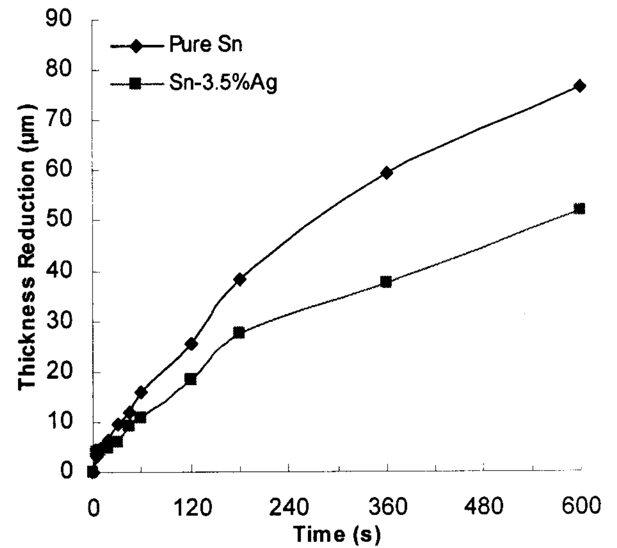

(d) 300 °C

Figure 5.4: Charts showing difference in copper thickness reduction for pure Sn and Sn-Ag solders during dipping process.

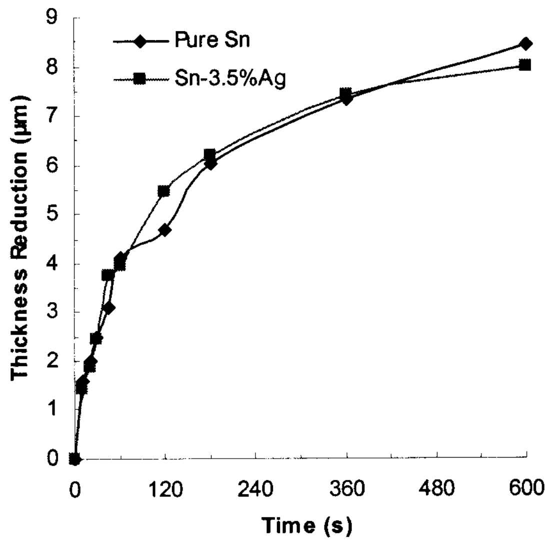

(a) At the melting points of two solders

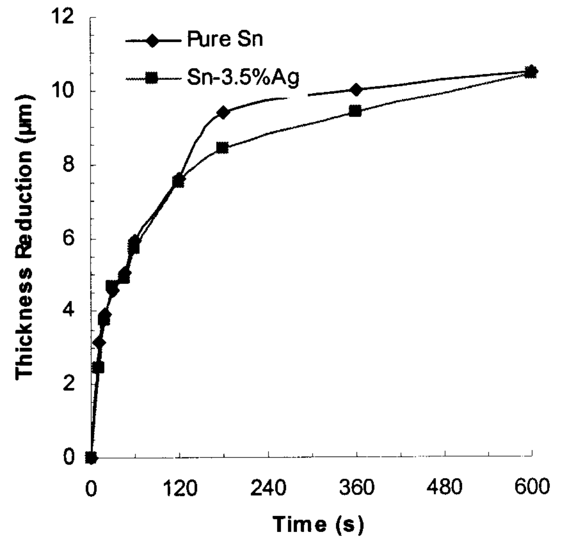

(b) 250 °C

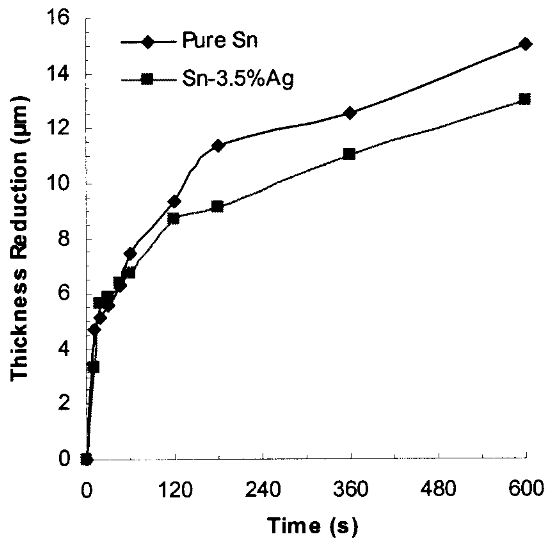

(c) 275 °C

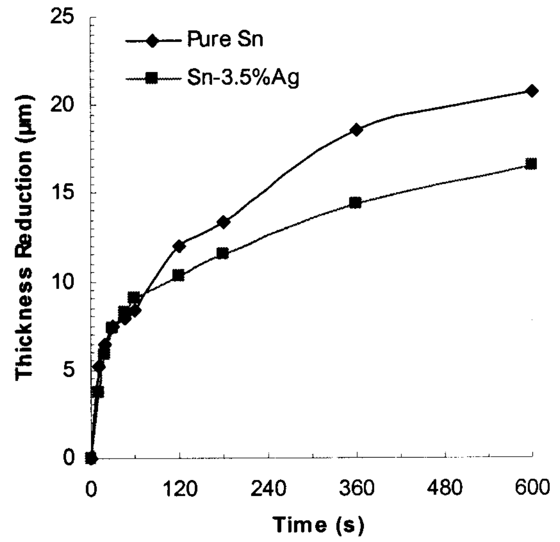

(d) 300 °C

Figure 5.5: Charts showing difference in copper thickness reduction for pure Sn and Sn-Ag solders during reflow process

CHAPTER - 6

KINETIC ANALYSIS OF GROWTH AND DISSOLUTION DATA

6.1 Kinetics of Intermetallic Compound Growth

The kinetics of growth of IMC for can be quantified based on average IMC thickness measurement. A simple power law is applicable for the growth of the intermetallic compound layer, both for dipping and reflow process. The IMC thickness can be related to dwell time as follows [1,2,9,12,13]

$$x(T, t) = Dt^n \tag{1}$$

where x is the thickness of the IMC layer, t is the dwell time, T is the temperature of molten solder, D is the diffusion coefficient, and n is a constant. The diffusion coefficient, D is related to temperature through an Arrhenius type equation as:

$$D = D_0 \exp(-Q_g / RT) \tag{2}$$

where D_0 is a pre-exponential temperature-independent constant, Q_g is the apparent activation energy for the layer growth into solute (copper in this case), and R is the universal gas constant.

The values of D_0, Q_g and n for each solder material were obtained by multivariable linear regression of experimental data of IMC growth during dipping and reflow process, using Arrhenius type equation (Figure 6.1, 6.2). The estimated values

were then used to fit the IMC thickness data as shown by the solid lines in Figure 4.5 and Figure 4.9 at each temperature for D and n as a function of T. The estimated values of D_0, Q_g and n for the two solders together with data available in open literature [1,2] are summarized in Table 6.1.

Table 6.1: Estimated values of IMC growth parameters

Solder Composition	Process	Q_g (Kj/mol)	D_o (μm/min)	n
Pure Sn	Dipping	8.14	7.34	0.10
Sn-3.5wt% Ag	Dipping	5.53	4.59	0.13
Pure Sn	Reflow	14.61	43.73	0.32
Sn-3.5wt% Ag	Reflow	13.83	49.88	0.32
Sn-3.5wt%Ag [1]* (221 °C – 251 °C)	Reflow	7.6	11.3	0.33
Sn-3.5wt%Ag [1]* (251 °C – 292 °C)	Reflow	24.7	574.7	0.33
Sn-Pb [2]*	Reflow	7.04	7.75	0.25

* As found in literature

Although the value of activation energy for the growth of IMC found in this study (Table 6.1) is lower than those available in the literature [1,2], the values of the activation energy for growth, Q_g and pre-exponential constant, D_0, are comparable with those obtained by Chada et al. [1] for Sn-3.5%Ag, and Shaffer et al. [2] for Sn-Pb, using reflow experiments of small solder samples. Activation energy for the growth of IMC is highly dependent on the type of process and the solder material. Chadha et. al. analyzed the overall reflow process in two stages depending on the reflow temperature. They found different values as given in Table 6.1 for the growth activation energy for the two

temperature ranges. In the present study, the reflow process was analyzed in one single stage starting from the melting temperature of the solder and reaching up to 300 °C. Since the value of Q_g estimated in this study falls in between the values found by Chadha, it is in agreement with their study. The Arrhenius plots for the two solders developed on the findings of the present study are compared with the data available in literature [1,2,25] in Figure 6.3.

It was observed that the dipping process yielded lower value of activation energy for IMC growth as compared to reflow process. The lower energy in dipping is also a result of the difference in the two soldering methods. In case of dipping process, since a large quantity of solder was already maintained at the experiment temperature, dissolution of copper and formation of IMC started immediately after the copper substrate was dipped. However, in case of reflow process, it took a finite time for the solder to attain the desired experiment temperature thus slowing down the rate of copper dissolution and IMC formation.

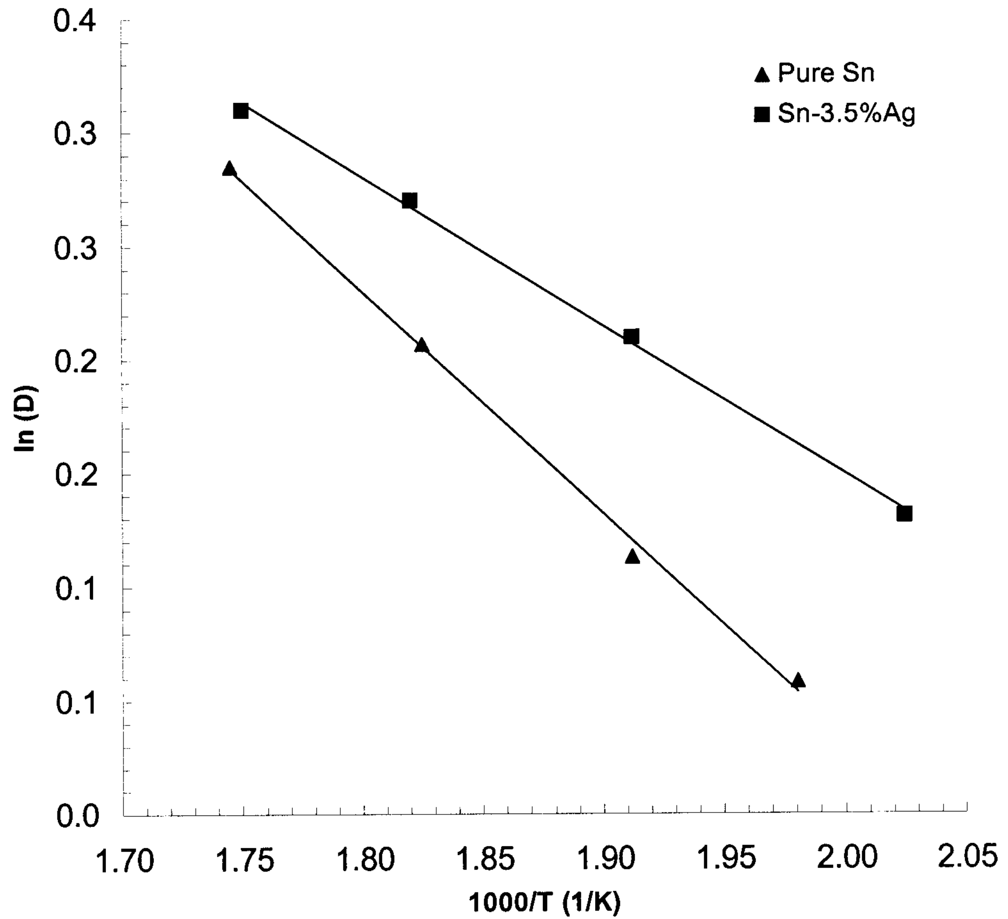

Process	Dipping
Analysis	IMC Growth

Figure 6.1: Arrhenius plot of *D* values obtained from the curve fits in Figures 4.9 (a) and (b)

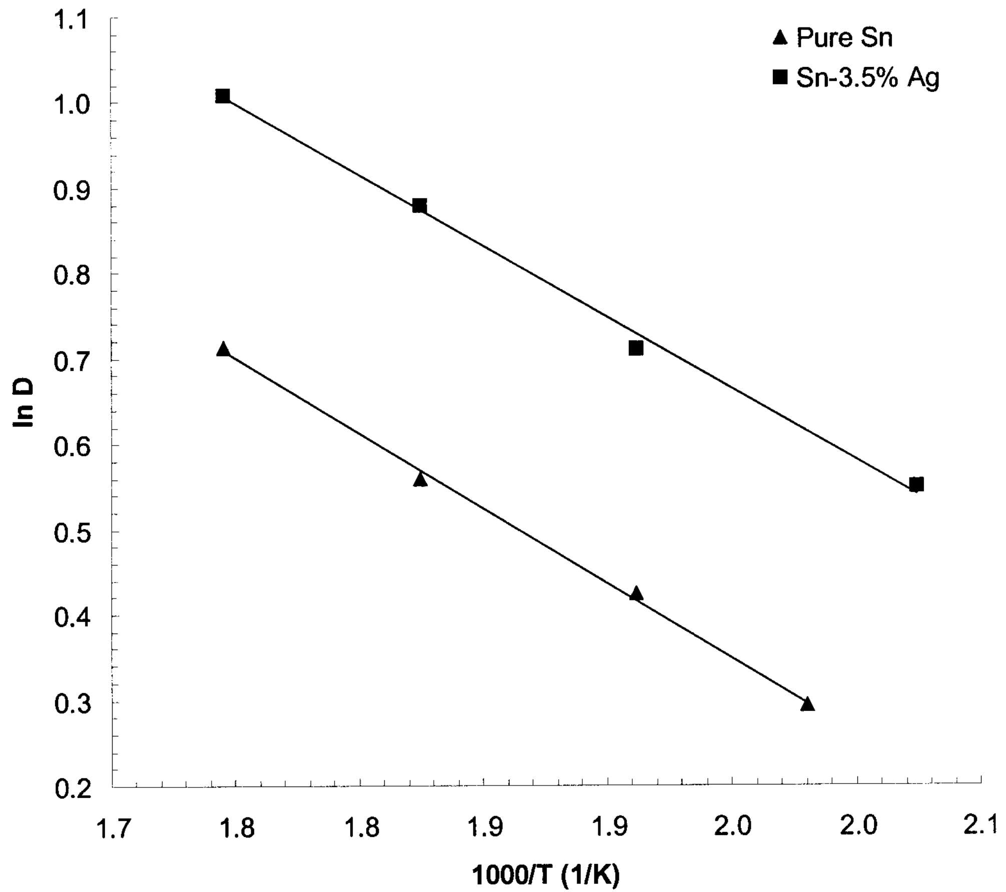

Process	Reflow
Analysis	IMC Growth

Figure 6.2: Arrhenius plot of *D* values obtained from the curve fits in Figure 4.9 (a) and (b)

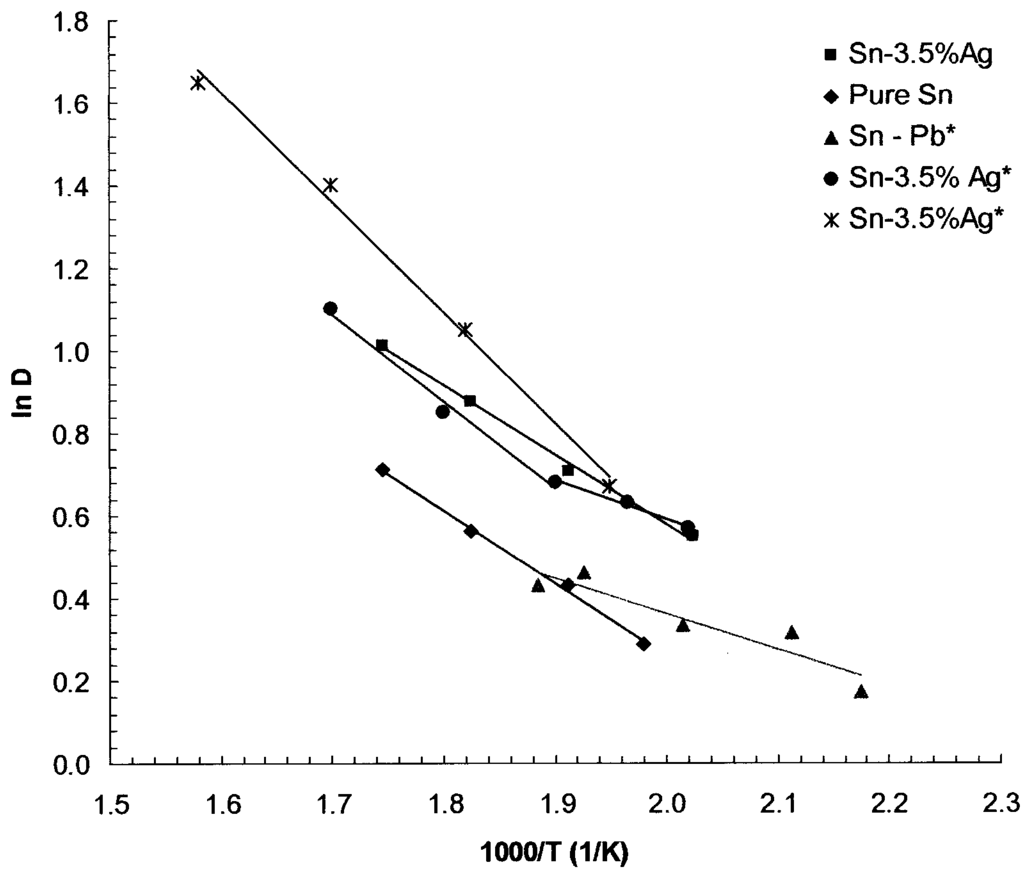

*As found in literature [1,2,25]

Figure 6.3: Comparison of the Arrhenius plots for IMC growth during reflow process

6.2 Kinetics of Copper Dissolution

It was assumed that the reduction in thickness of the copper substrate is a direct and good estimation of the total copper dissolved into liquid solder. A similar power law as given in equation (1) governs the total dissolution of copper into liquid solder as.

$$x(T, t) = Dt^n \tag{3}$$

where x is the reduction in thickness of copper substrate and a measure of total copper dissolution, t is the dwell time and T is the solder temperature.

Also,

$$D = D_0 \exp(-Q_d / RT) \tag{4}$$

where Q_d is the apparent activation energy for copper dissolution. The values of D_0, Q_d and n for each solder material were established both for dipping and reflow process by multivariable linear regression analysis of experimental data of thickness reduction, using Arrhenius type equation (Figure 6.4 and 6.5). The estimated values were then used to fit the thickness reduction data as shown by the solid lines in Figures 5.1 and 5.2 at each temperature for D and n as a function of T. Table 6.2 summarizes the growth kinetics parameters for copper dissolution in molten solders.

Table 6.2: Estimated values of parameters for copper dissolution

Solder Composition	**Process**	Q_d (kJ/mol)	D_o (μm/min)	**n**
Pure Sn	Dipping	28.0	6157.0	0.67
Sn-3.5wt% Ag	Dipping	26.10	2981.0	0.63
Pure Sn	Reflow	28.15	3576.0	0.32
Sn-3.5wt% Ag	Reflow	21.31	714.0	0.32

The apparent activation energy for dissolution of copper was determined to be higher for pure Sn than Sn-Ag both for dipping and reflow process. The high activation energy for pure Sn could be due to its higher melting temperature (223 °C) as compared to Sn-3.5%Ag (221 °C).

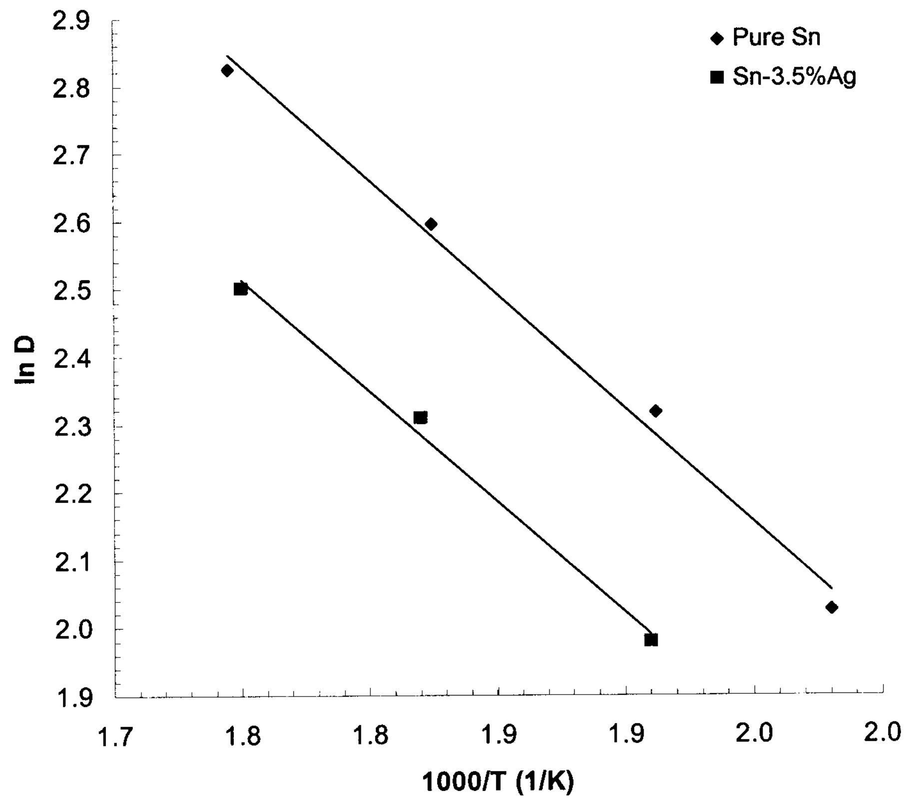

Process	Dipping
Analysis	Copper Dissolution

Figure 6.4: Arrhenius plot of *D* values obtained from the curve fits in Figures 5.1 (a) and (b)

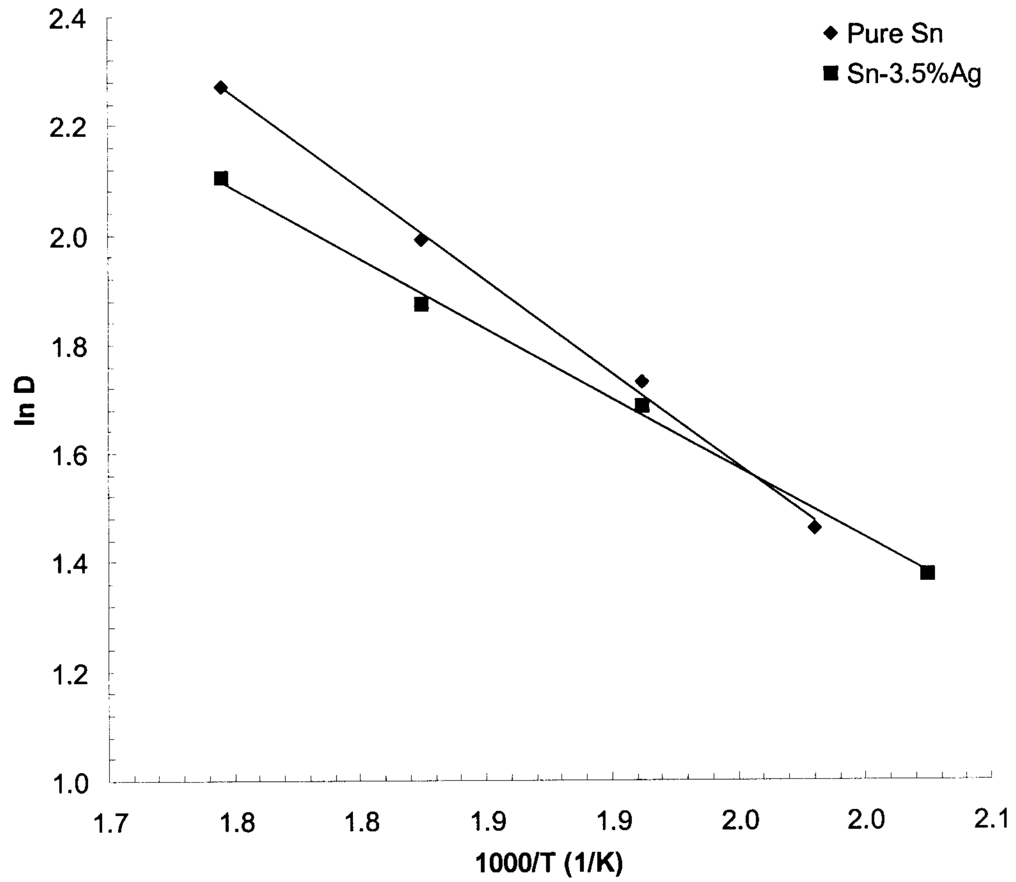

Process	Reflow
Analysis	Copper Dissolution

Figure 6.5: Arrhenius plot of *D* values obtained from the curve fits in Figures 5.2 (a) and (b)

CHAPTER - 7

CONCLUSIONS

In the present study, the dissolution of copper and growth of Cu-Sn intermetallic compound at the solder-copper interface, during soldering process, was investigated. The phenomenon was analyzed as function of dwell time and temperature of solder for two different solders, the pure Sn and Sn-3.5wt%Ag. Kinetic analysis of the copper dissolution and IMC growth data was performed and related parameters were obtained. The findings of the study are summarized in the following lines.

1. Dissolution of copper and growth of intermetallic compound is a strong function of solder temperature and dwell time.
2. Copper dissolution and IMC growth are favored by increasing solder temperature.
3. Rate of copper dissolution and IMC growth is high at the initial stage of the process but tends to be constant at the terminal stages.
4. Dissolution of copper was observed more in pure Sn than Sn-Ag solder implying that the addition of Ag aids in retarding the copper dissolution.
5. Sn-Ag showed lower activation energy for copper dissolution and IMC growth than pure Sn.
6. Both solders revealed scalloped morphology for IMC, but the scallops were round in pure Sn and needle-like in Sn-Ag.
7. Copper dissolution and IMC growth data were fitted with equation, $x = Dt^n$ and demonstrated a good fit with rms value in the range 0.96 to 0.98.

CHAPTER 8

SCOPE FOR FURTHER WORK

The present study can possibly be extended in the following directions.

1. Study the behavior of the IMC by adding micro and nano size copper particles in the solders.
2. Develop a numerical model for the overall process of copper dissolution and IMC growth.
3. Study of the strength of soldered joints under thermal and mechanical fatigue.
4. Behavior of different solders under different service environments.

REFERENCES

1. S. Chada, W. Laub, R. A. Fournelle, and D. Shangguan (1999) "An Improved Numerical Method for Predicting Intermetallic Layer Thickness Developed during the Formation of Solder Joints on Cu Substrates," *J. Electron. Mater.,* Vol. 28: 1194-1202.

2. M. Shaefer, W. Laub, J. M. Sabee, and R. A. Fournelle (1996) "A Numerical for Predicting Intermetallic Layer Thickness Developed During the Formation of Solder Joints," *J. Electron. Mater.,* Vol. 25: 992-2003.

3. M. Shaefer, R. A. Fournelle, and J. J. Liang (1998) *J. Electron. Mater.,* Vol. 27: 1167-.

4. O. Fouassier, J. Chazeals, and J. Silvan (2002) "Conception of a consumables copper reaction zone for a NiTi/SnAgCu composite material," *Composites: Part A*, Vol. 33: 1391-1395.

5. D. Ma, W. D. Wang, and S. K. Lahiri (2002) "Scallop formation and dissolution of Cu-Sn intermetallic compound during solder reflow," *J. Appl. Phys.*, Vol. 91: 3312 – 3317.

6. H. K. Kim and K. N. Tu (1995) "Rate of consumption of Cu in soldering accompanied by ripening," *Appl. Phys. Lett.* Vol. 67: 2002 – 2004.

7. Y. G. Lee, and J. G. Duh (1998) "Characterizing the formation and growth of intermetallic compound in the solder joint," *J. Mater. Sc.* Vol. 33: 5569 – 5572.

8. T. M. Korhonen, P. Su, S. J. Hong et. al. (2000) "Reaction of Lead-Free Solders with CuNi Metallizations," *J. Electron. Mater.*, Vol. 29: 1194 – 1199.

9. K. Suganuma (2001) "Advances in lead-free electronics soldering," *Current Opinion in Solid State and Materials Science,* Vol. 5: 55 – 64.

10. S. W. Chen and Y. W. Yen (1999) "Interfacial Reaction in Ag-Sn/Cu Couples," *J. Electron. Mater.,* Vol. 28: 1203 – 1208.

11. Y. C. Chan, C. K. Alex, and J. K. L. Lai (1998) "Growth kinetic studies of Cu-Sn intermetallic compound and its effect on shear strength of LCCC SMT solder joints," *Mat. Sc. Eng. B*, Vol, B55: 5 – 13.

12. K. H. Prakash and T. Sritharan (2001) "Interface Reaction Between Copper and Molten Tin-Lead Solders," *Acta Mater.*, Vol. 49: 2481 – 2489.

13. Y. G. Lee and J. G. Duh (1999) "Interfacial morphology and concentration profile in the unleaded solder/Cu joint assembly," *J. Mater. Sc.,* Vol. 10: 33 – 43.

14. Rudolf Strauss (1994) "Surface Mount Technology," Butterworth-Heinemann Ltd.

15. Giles Humpston, David M. Jacobson (1993) "Principles of Soldering and Brazing," *ASM International.*

16. Donald P. Seraphim, Ronald C. Lasky and Che-Yu Li (1989) "Principles of Electronic Packaging," McGraw-Hill Book Company.

17. Armin Rahn (193) "The Basics of Soldering," John Wiley & Sons Inc.

18. A. J. Sunwoo, J. W. Morris, Jr., and G. K. Lucey, Jr. (1992), *Metall. Trans.* A:23: 1323.

19. A. J. Sunwoo, H. Hayashigaani, J. W. Morris, Jr., and G. K. Lucey, Jr. (1991), *JOM* 43 (6): 21.

20. K. N. Tu, T. Y. Lee, J. W. Jang, L. Li, D. R. Frear, K. Zeng and J. K. Kivilahti (2001) "Wetting reaction versus solid state aging of eutectic SnPb on Cu" *J. of Appl. Phys.* 89: 4843-4849.

21. A. S. Zuruzi, C.-h. Chiu, S. K. Lahiri, and K. N. Tu (1991) "Roughness evolution of Cu_6Sn_5 intermetallic during soldering" *J. of Appl. Phys.* 86: 4916-4921.

22. G. Ghosh (2000) "Coarsening kinetics of Ni_3Sn_4 scallops during interfacial reaction between liquid eutectic solders and Cu/Ni/Pd metallization" *J. of Appl. Phys.* 88: 6887-6897.

23. B. J. Lee, N. M. Hwang and H. M. Lee (1997) "Prediction of interface reaction products between Cu and various solder alloys by thermodynamic calculation" *Acta Mater.* 45: 1867-1874.

24. L. A. Clevenger, B. Arcot, W. Ziegler, E. G. Colgan, Q. Z. Hong, F. M. d'Heurle, C. Cabral, Jr., T. A. Gallo, and J. M. E. Harper (1998) "Inter-diffusion and phase formation in Cu(Sn) alloy films" *J. of Appl. Phys.* 83: 90-99.

25. J. London and D. W. Ashall, (1986), *Brazing and Soldering* 11: 49.